NASA TECHNICAL NOTE

NASA TN D-6360

JAN 2 1

COMBUSTOR LINER FILM COOLING IN THE PRESENCE OF HIGH FREE-STREAM TURBULENCE

by Albert J. Juhasz and Cecil J. Marek

Lewis Research Center
Cleveland, Ohio 44135

CONTENTS

COMBUSTOR LINER FILM COOLING IN THE PRESENCE OF HIGH

FREE-STREAM TURBULENCE

by Albert J. Juhasz and Cecil J. Marek

Lewis Research Center

SUMMARY

Liner film cooling experiments with various slot configurations were conducted in a rectangular section of a gas turbine combustor operated at 1 atmosphere inlet pressure and up to 2000° F (1367 K) outlet temperature. The experimental cooling effectiveness data were compared to values predicted by several correlations currently in use. Experimental film cooling effectiveness values were found to be almost an order of magnitude lower than some of the predictions, with film mass flow rate and hot stream turbulence level being more important correlating parameters than slot geometry. In an effort to improve prediction accuracy a turbulent mixing model was developed, wherein the turbulence level of the hot gas stream is considered. Assuming a turbulent mixing level of 0.15 for the combustor tested, this model correlated experimental film cooling effectiveness values within ±20 percent. The corresponding wall temperature errors were ±20 percent or less, with the errors decreasing to less than ±10 percent at the higher wall temperatures. The data of Eckert and Birkebak and the data of Hatch and Papell were also correlated by assuming a turbulent mixing level of 0.01, a value which is compatible with the low turbulence test ducts used in these references.

INTRODUCTION

In the design of high performance gas turbine combustors it is important to keep the quantity of air used for liner film cooling as small as possible. To do this effectively, a method of predicting the film cooling flow requirements is needed. Several such methods do exist based on empirical correlations of which a few are considered in this report (refs. 1 to 6). Most of the data used in developing these correlations, however, were obtained under conditions not present in actual gas turbine combustors. For example, test flow ducting was sometimes designed to insure flows of low turbulence level. Con-

tinuous slots were used without the support obstructions present in actual combustor cooling slots, and hot gas to cooling film temperature differences were lower than the differences that frequently exist in actual combustors.

Such idealized conditions resulted in cooling effectiveness values that might be expected to be higher than those achieved in actual combustor cooling applications. The high degree of nonuniformity in typical combustor flow fields could disturb the cooling film excessively and reduce the cooling effectiveness. Therefore, a program was undertaken to obtain film cooling data in a true gas turbine combustor environment.

Tests were conducted in a high performance rectangular combustor described in the APPARATUS section of this report. A variety of slot configurations were used. The film effectiveness data obtained were compared to results predicted by the correlations of references 1 to 6. Because of the lack of agreement between experimental film cooling effectiveness data and values predicted by the aforementioned correlations a simple mixing model is developed in the ANALYSIS section. The model incorporates the mainstream turbulence level which must be estimated for a given application.

SYMBOLS

A_s film slot flow area

a   mixing coefficient used in eq. (21)

C_m turbulent mixing coefficient or turbulent mixing level

C_p specific heat

D_H hydraulic diameter

f   function defined by eq. (15)

h   heat transfer coefficient defined in table III

k   thermal conductivity

L   width of cooling slot

M   mass flux ratio, $\rho_s U_s / \rho_H U_H$

$\mathcal{M}_H$ Mach number of hot gas stream

m   viscosity-temperature exponent in eq. (22)

m_E' mass entrained into cooling film per unit area per unit time

m_F mass flow rate of film at any x

m_H mass flow rate of hot gas stream

m_s	mass flow rate of film at slot
P	pressure
Pr	Prandtl number
Re	Reynolds number
s	equivalent slot height, A_s/L
T_{AW}	wall temperature without film cooling
T_F	temperature of film stream at any x
T_H	hot gas temperature
T_s	film temperature at slot
T_W	wall temperature
U_H	hot gas stream velocity
U_s	film velocity at slot
$\left.\begin{array}{c} \overline{u'^2} \\ \\ \overline{v'^2} \\ \\ \overline{w'^2} \end{array}\right\}$	time averages of three components of turbulent velocity fluctuations
W_H	maximum weight flow rate of hot gas stream
W_s	weight flow rate of film at slot
X	distance parameter defined in table II
X_1	film cooling parameter defined in table II
x	distance downstream from slot
y	distance normal to x
α	thermal diffusivity, $k/\rho C_p$
γ	specific heat ratio
η	film cooling effectiveness defined by eq. (1)
μ	viscosity
ρ	mass density
τ	turbulence intensity or turbulence level, percent

Subscripts:

calc	calculated

e   local conditions along outer edge of boundary layer

f   properties evaluated at $(T_H + T_s)/2$

H   hot gas conditions

inlet   inlet conditions

meas   measured

o   property at stagnation conditions

s   slot conditions

x   based on downstream distance x

ANALYSIS

The major mechanism for heat transfer in the current tests was turbulent convection to the film cooling layer. A simple model was developed by Stollery and El-Ehwany (ref. 2), which makes the following assumptions:

(1) The temperature of the film at any downstream location x is equal to the wall surface temperature at x.

(2) The axial pressure drop in the film is negligible.

(3) The change in specific heat C_p with temperature is small.

(4) The hot stream and film composition is the same.

(5) The hot gas temperature T_H is constant.

With these assumptions, they showed that the film cooling effectiveness is given by

$$\eta = \frac{T_H - T_W}{T_H - T_s} = \frac{m_s}{m_F} \tag{1}$$

where m_s is the mass flow rate injected from the slot and m_F is the total mass flow rate of the film at any distance x downstream from the slot exit. The value m_F includes the initial mass rate and the entrainment rate into the film as indicated in figure 1, that is,

$$m_F = m_s + L \int_0^X m_E' \, dx \tag{2}$$

Previous investigators, Eckert and Birkebak (ref. 1) as well as Stollery and El-Ehwany (ref. 2) obtain m_F, the total mass of the film cooling layer, by assuming the film grows

4
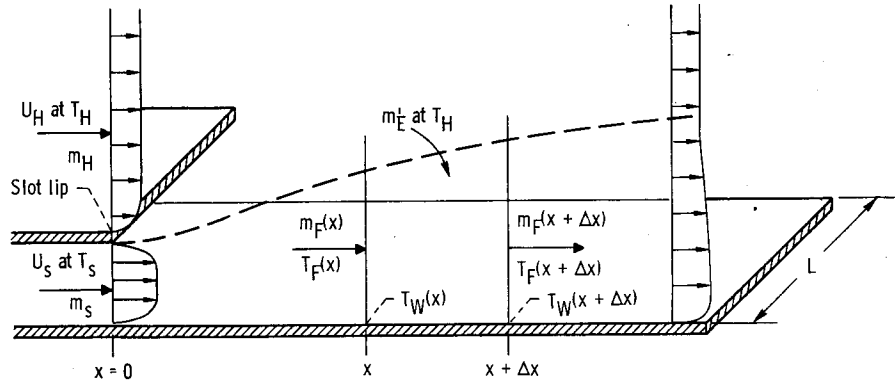
Figure 1. - Control volume for one-dimensional entrainment model used in turbulent mixing film cooling correlation.

at the same rate as a developing boundary layer on a flat plate. They obtain an expression which works well far from the slot exit, typically at x/s values greater than 60, but which does not correlate the data well close to the slot exit.

In the model introduced in this study it is assumed that the entrainment rate per unit area of the film cooling stream is directly proportional to the main stream mass flux, that is,

$$m_E' = C_m \rho_H U_H \tag{3}$$

where C_m is a mixing coefficient. Furthermore, C_m is related to the turbulence intensity by assuming that the entrainment rate is proportional to the y component of the fluctuating hot gas velocity $\sqrt{\overline{v'^2}}$, that is,

$$m_E' = \rho_H \sqrt{\overline{v'^2}} \tag{4}$$

For the special case of isotropic turbulence, the mean fluctuations in the three components are equal, that is,

$$\overline{u'^2} = \overline{v'^2} = \overline{w'^2}$$

Defining the intensity of turbulence τ by the following equation:

$$\tau = \frac{\sqrt{\overline{u'^2}}}{U_H} \times 100 \tag{5}$$

5

results in the mixing coefficient becoming

$$C_m = \frac{\tau}{100} \tag{6}$$

The mixing coefficient C_m may also be a function of other variables such as the scale of turbulence, the angle of blowing of the film cooling stream, the velocity differences between the film and the mainstream, as well as hot gas acceleration. These latter effects tend to increase C_m beyond the value given by equation (6). For combustors where turbulence is high the relative effects of the latter variables are small.

The film cooling effectiveness can then be written after equations (2) and (3) are substituted into equation (1), with the assumption that $C_m \rho_H U_H$ is constant, as

$$\eta = \frac{1}{1 + C_m \dfrac{x}{Ms}} \tag{7}$$

Equation (7) represents the basic turbulent mixing correlation. When the cooling film and the hot gas stream are not of the same general composition, the effect of differences in heat capacity cannot be neglected. The correlation then becomes

$$\eta = \frac{1}{1 + C_m \dfrac{x}{Ms} \dfrac{C_{p_H}}{C_{p_S}}} \tag{8}$$

The effect of changes in C_m (as due to a change in the percent turbulence) is shown in figure 2 for two ranges of downstream distance parameter x/Ms. The model indicates that the effect of free-stream turbulence is an important factor in correlating the film cooling effectiveness. The film cooling stream is more effective for smaller values of the mixing coefficient C_m. For a specific value of C_m, the mass flow rate of cooling air required to obtain a given film cooling effectiveness at a specific distance can be obtained from figure 2 or equation (7) with sufficient accuracy for most applications. Where additional computational accuracy is warranted or in cases where binary gas streams are used (ref. 3), equation (8) applies.

6
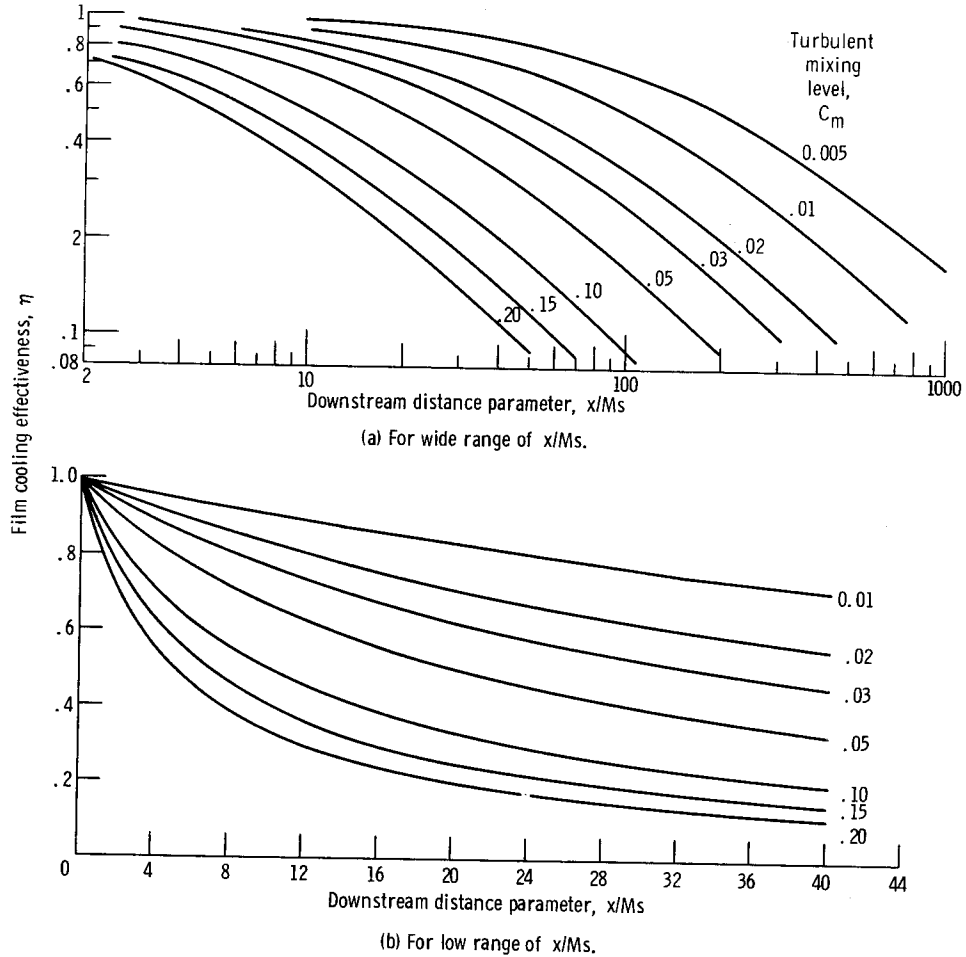
Figure 2. - Turbulent mixing correlation: effect of mixing coefficient C_m on film cooling effectiveness η.

APPARATUS AND INSTRUMENTATION

Flow System

The rectangular combustor test rig and associated airflow systems are shown schematically in figure 3. Ambient temperature combustion airflow at 10 atmospheres nominal pressure was measured by a sharp-edged orifice installed according to ASME standards. The air then entered a direct fired preheater using ASTM A-1 fuel where the temperature was increased to 600° F (589 K). A plenum chamber insured a well mixed flow at the test combustor inlet. The test combustor was fitted with a special adapter flange which permitted metered film cooling air to be brought into the chamber from a separate line through a series of valves permitting accurate pressure and flow control. Immediately downstream of the combustor, an instrument section housed seven five-
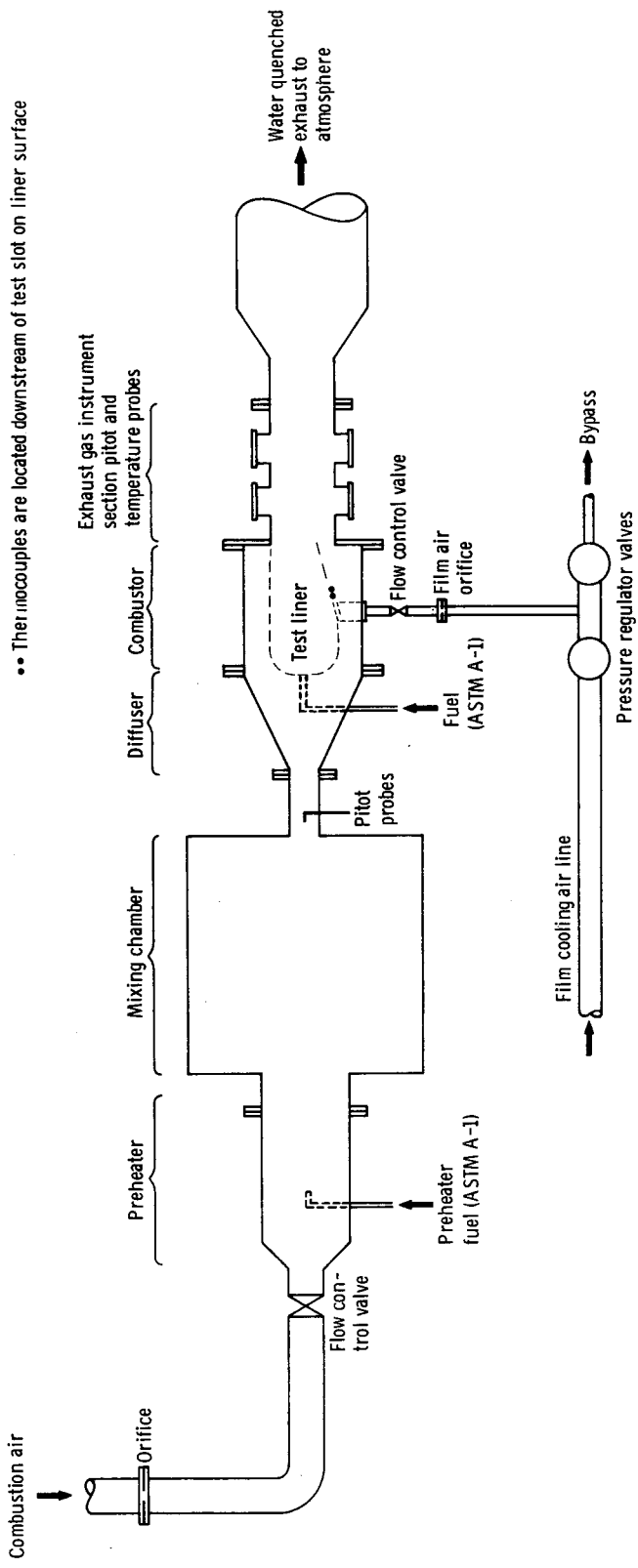
Figure 3. - Combustor test setup (schematic of flow system).
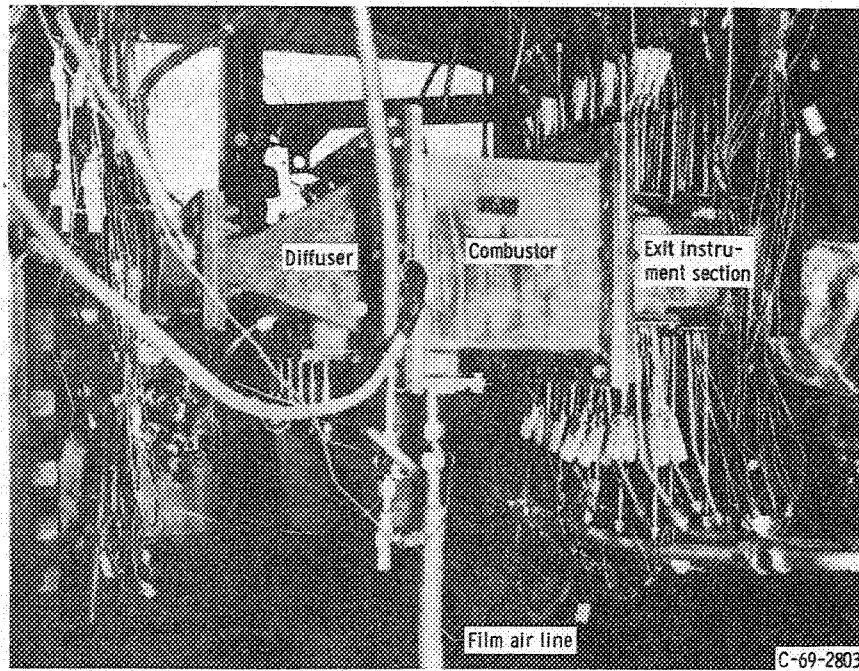
Figure 4. - Test combustor installed in flow system.

point total pressure rakes and eight five-point bare wire platinum-platinum-13 percent rhodium thermocouple rakes for monitoring combustor exhaust conditions. A more detailed description of the combustor exit instrumentation is given in reference 7. The flow was finally exhausted through a water quench scrubber to the atmosphere. Figure 4 is a photograph of the combustor rig showing the major components.

Test Combustor

A rectangular side-entry-type combustor was used to provide the hot gas environment for the film cooling study. The design and performance of various side-entry-type combustor models was reported in reference 7. Figure 5 shows two views of the model used as the test combustor including the alterations necessary for this study.

As shown in figure 5, about 85 percent of the airflow is introduced into the combustion chamber through two rows of scoops in the upper liner. This upper liner represents the outer liner in an annular configuration of this design. The first row of scoops ducts about 25 percent of the total airflow into the combustor; the second row, about 60 percent. About 10 percent of the air enters through the dome, including the airflow through the fuel nozzle swirlers. In the original design about 5 percent of the airflow is used
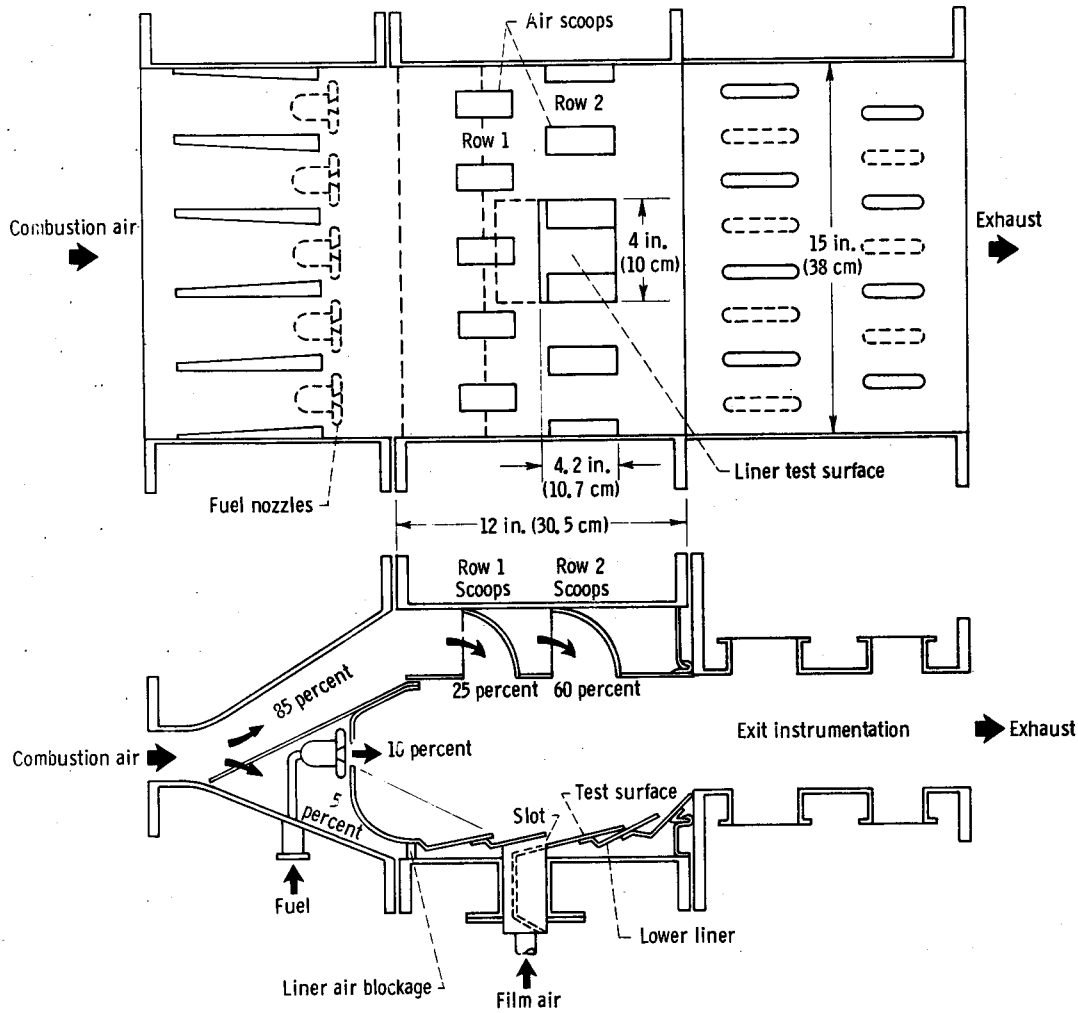
Figure 5. - Test combustor with alterations for film cooling study.

for cooling the lower liner, that is, the inner liner in an annular configuration. The combustor was fired with ASTM A-1 fuel.

To achieve controlled conditions during the film cooling tests, certain alterations were made on the lower liner and the combustor housing. A 4- by 4.2-inch (10- by 10.7-cm) section was removed from the segmented lower liner central area and replaced with a continuous flat sheet which became the test surface. The material used for this modified lower liner was 0.062-inch (0.16-cm) stainless steel (SS 304). The combustor casing was modified by the addition of a flanged rectangular opening to its lower wall. This opening permitted metered external film cooling air to be blown over the test surface by use of an air supply box designed for this purpose. To insure that the metered external film air supplied through this box was the only source of lower liner cooling, the normally required 5 percent liner cooling air was blocked by placing a wall between

10

the casing and the upstream end of the lower liner. This change did not result in signif-icant warpage of the test surface after it was exposed to the hot gas stream.

Effects of Combustor Airflow Distribution

As discussed in the previous section and indicated in figure 5, the second row of scoops in the upper liner turns approximately 60 percent of the airflow into the chamber. The significant fact to note is that this air is discharged normal to and directly above the test surface. If it is assumed that the flow from the scoops is uniformly distributed, the hot gas flow is thus linearly increasing from 40 to 100 percent of total flow between the upstream and downstream ends of the test surface.

Moreover, a 15 percent reduction in cross-sectional area of the chamber experi-enced by the hot gas flowing over the test surface causes additional acceleration of the main stream. These combined effects of mass addition and area change cause the hot stream mass flux to increase by a factor of 2. 1 between the 1- and the 4-inch (2. 5- and 10. 2-cm) stations along the test surface.

Finally the jets of air blown into the chamber by the scoops cause a significant in-crease in the hot stream turbulence level because of the deep jet core penetration and large turning vortices.

These effects contribute to the more rapid breakdown of the protective cooling film than is the case in nonaccelerating low turbulence flow. Hence, they were taken into account in the analysis of data.

Slot Geometries Tested

As indicated in the previous section, external film cooling air was injected over the test surface by use of a specially designed box. This device could be inserted into the chamber through a flanged opening in the lower wall of the combustor casing, as shown in the lower views of figures 5 and 6. The metered external film cooling air was sup-plied through a 1-inch- (2. 5-cm-) diameter tube. The flow was then expanded to fill a 0. 4- by 3. 9-inch (1- by 9. 9-cm) passage. This flow area was continued through an 80$^{\text{o}}$ turn to discharge the flow parallel to the test surface. To obtain a smooth cooling film, the position of the box could be adjusted on assembly so that the lower wall of the pas-sage, at its discharge opening, fit snugly against and flush with the upstream edge of the test surface. The discharge opening of the box could be altered by mounting inserts of various shapes into it, thus changing the slot geometry.

The various insert designs used to modify the discharge slot geometry of the film
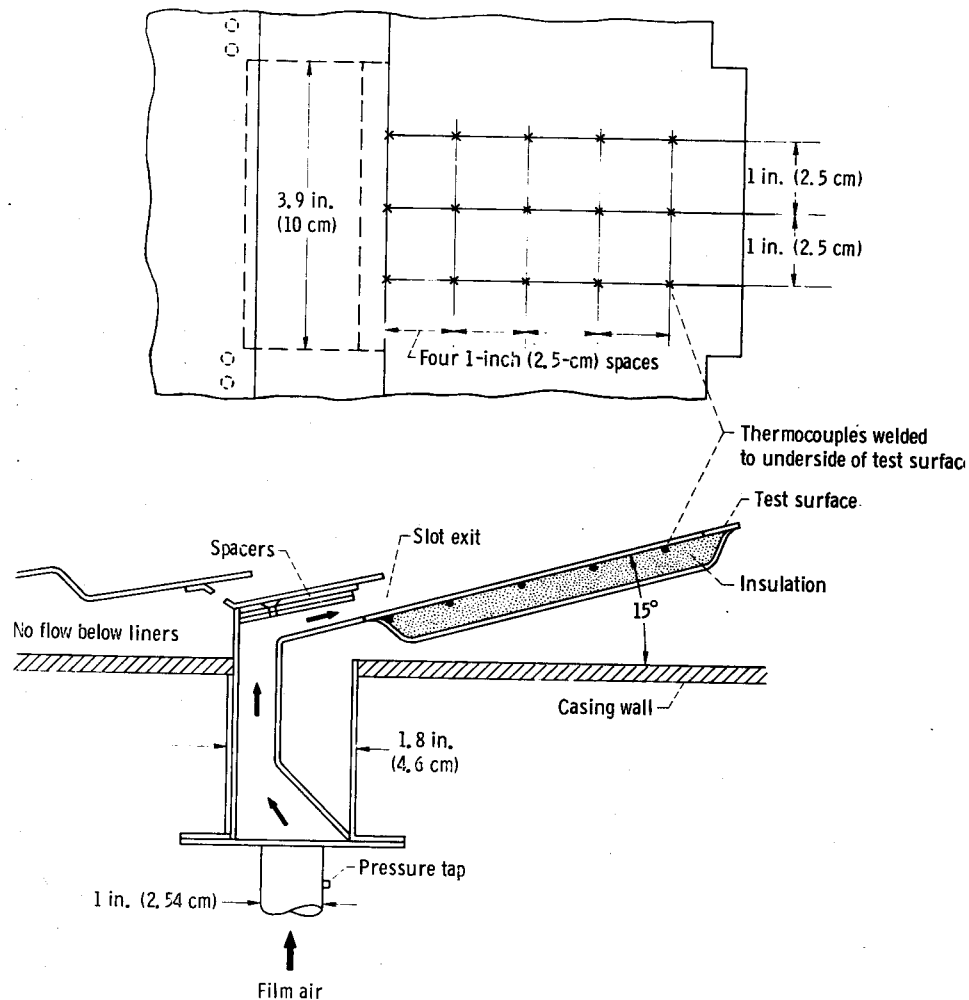
Figure 6. - Test liner surface showing location of thermocouples and film air supply box.

air supply box are listed and sketched in table I. The first four geometries shown are continuous or unobstructed slots. The only characteristic varied between configurations 1 to 3 was the slot height. As shown in figure 6, this was done by fastening flat spacers to the upper slot wall. The sketch in table I shows that this technique resulted in a blunt discharge lip for configuration 3. In an attempt to evaluate the effect of this blunt lip on the film cooling effectiveness, configuration 4 was also tested. In configuration 4 the spacers were fastened to the lower wall of the slot thus raising the discharge opening 0.25 inch (0.63 cm) above the test surface.

Configurations 5 to 9 were "supported" slots, representative of those found in actual combustor liners. In these the film flow area was formed by a series of holes drilled into the support spacer as shown. For these geometries the size and spacing of the flow holes was varied. Also varied was the angle relative to the liner surface at which the

12

TABLE I. - SLOT GEOMETRIES TESTED

Configuration number	Description	Open area		Sketch of slot
		in.^{2}	cm^2	
1	0.3-Inch (0.76-cm) continuous slot	1.17	7.6	
2	0.156-Inch (0.4-cm) continuous slot	0.61	3.9	
3	0.062-Inch (0.16-cm) continuous slot	0.245	1.58	
4	0.062-Inch (0.16-cm) continuous slot raised 1/4 inch (0.64 cm) above surface	0.245	1.58	
5	Eight 1/4-inch (0.64-cm) holes at 45°	0.392	2.52	
6	Four 1/4-inch (0.64-cm) holes at 45°	0.196	1.26	
7	19 1/16-inch (0.16-cm) holes at 45°	0.058	0.37	
8	Eight 3/16-inch (0.48-cm) holes at 0°	0.221	1.42	
9	Eight 3/16-inch (0.48-cm) holes at -45°	0.221	1.42	
10	Wiggle strip in 0.3-inch (0.76-cm) slot	0.98	6.3	

13

cooling air was discharged. It should be noted that, in configurations 5, 6, and 7, in which the cooling air is initially discharged at 45° above the test surface, it will still flow parallel to the surface after it emerges from the slot. This is because the film impacts on the upper trailing lip of the slot which then turns it in a direction parallel to the test surface. This film cooling slot design has been used successfully in existing axially segmented liners. The main advantage of this design is that, in addition to cooling the downstream surface, the cooling air also provides effective impingement cooling for the upper lip of the slot. Configurations 8 and 9, with holes at 0° and -45°, were tested for the purpose of obtaining comparison data to the 45° hole geometries.

In configuration 10, the support between the upper and lower slot walls was provided by a sheet metal strip, shaped as shown. Such a strip is commonly referred to as a "wiggle strip." Configuration 10 combines the advantages of high open area and structural rigidity.

Test Surface Instrumentation

As illustrated in figure 6 the underside of the test surface, extending for 4.2 inches (10.7 cm) immediately downstream of the film air box discharge opening, was instrumented with fifteen Chromel-Alumel thermocouples. These were tack welded on the surface in five rows spaced 1 inch (2.5 cm) apart in the downstream direction. There were three thermocouples to each row, also spaced at 1-inch (2.5-cm) intervals, so that the middle thermocouple was alined with the axial center of the 4-inch- (10-cm-) wide test surface. Four Chromel-Alumel couples were inserted 0.25 inch (0.6 cm) into the gas stream to measure film temperatures at the slot inlet and also at the downstream end of the test surface. The underside of the test surface was insulated with a 0.4-inch (1-cm) layer of Fiberfrax material (alumina-silica compound with $k = 0.08$ Btu/(hr)(ft)(°F) at 1400° F or 0.14 J/(sec)(m)(K) at 1033 K).

Figures 7(a) and (b) are photographs showing oblique top and bottom views of the test liner surface and its orientation relative to the major components of the combustion chamber. The thermocouples shown in figure 7(a) were used to measure gas temperatures both upstream and downstream of the test surface. Figure 7(b) shows the surface thermocouples mounted on the underside of the test surface prior to application of the insulating material. Both views further illustrate the location of the air scoops relative to the test surface. The effect of these scoops on the airflow distribution was described previously.

14

(b) Bottom side of liner test surface.

(a) Top side of liner test surface and its location relative to main combustion chamber components.

Figure 7. – Liner test surface.

15

Film Air Flow Measurement

A sharp-edged orifice installed according to ASME specifications was used to measure the film cooling air flow rate. The nominally ambient air temperature at the orifice was measured with an iron-constantan thermocouple. The upstream orifice pressure in the film cooling orifice line could be regulated from near atmospheric to 145 psia (100 N/cm^2 abs), thus permitting the film flow rate to be measured over a ten to one range with a single orifice plate. The upstream orifice pressure was measured with a high accuracy Bourdon-type gage. Vena contracta taps were used to determine the orifice pressure drop which was read on a 100-inch (254-cm) manometer filled with dibutyl phthalate fluid having a specific gravity of 1.04.

Measurement of Film Slot Pressure Drop

In order to obtain an estimate of the pressure drop required to force a given amount of film cooling flow through each of the slot configurations, a pressure tap was installed at the inlet of the film air supply box as shown in figure 6. Pressures measured at this tap were read on a dibutyl phthalate (specific gravity = 1.04) or mercury manometer. While these readings included the pressure drop of the airflow passage inside the box, the error was negligible for most slot configurations. For the high open area slot geometries the measured pressure drop values were corrected by subtracting the pressure drop computed for the supply box air passage.

TEST CONDITIONS AND PROCEDURE

Range of Test Conditions

The combustor was operated at near atmospheric pressure throughout the test program. The combustor inlet air temperature was 600° F (589 K) provided by an upstream direct fired preheater. Combustor reference velocities were 75 and 100 feet per second (23 and 30 m/sec). These reference velocities were computed from airflow rate, combustor inlet static pressure and temperature, and the maximum cross-sectional area of the combustor housing (1.04 ft^2 or 0.097 m^2). Average exhaust gas temperature settings were 600°, 1400°, 1600°, 1800°, and 2000° F (589, 1033, 1144, 1255, and 1367 K), with the greater part of the tests conducted at the highest temperature. Corresponding adiabatic wall temperatures on the test surface varied between 600° and 1900° F (589 and 1311 K). Combustion chamber hot gas velocity varied from 100 to 450 feet per second (30 to 135 m/sec). Cooling air temperatures at the discharge slot ranged from 150° to 400° F (339 to 478 K) and cooling air velocities from 50 to 1300 feet per second (15 to

16

390 m/sec). The nominal film flow to hot flow ratios were computed by dividing the total cooling air flow by that fraction (25 percent) of the hot gas flow which passed over the test surface. This fraction in turn was obtained by dividing the test surface width by the combustion chamber width and multiplying by a profile factor. Data were taken at nominal ratios of film flow to hot flow of 2, 4, 8, and 16 percent. The highest ratio was omitted for some of the small area slot configurations. The corresponding values of mass flux ratio M, ratio of film mass flow per unit flow area to hot gas flow per unit open area, ranged from 0.4 to 116.

Combustion Chamber Operation

A standard procedure was followed to insure constant combustion chamber conditions while liner film cooling data were taken. The direct fired preheater was set for a constant combustor inlet temperature of approximately 600° F (589 K). The desired combustor exit gas temperature, measured by the platinum-platinum-13 percent rhodium rakes at the burner exit section, and the combustor reference velocity were controlled as closely as possible by adjusting the combustion air mass flow rate and the combustor fuel air ratio. As indicated in the previous section, the greater part of the data were obtained at a combustor exit temperature of 2000° F (1367 K) and a combustor reference velocity of 100 feet per second (30 m/sec). However, to broaden the scope of the data, one slot geometry was also tested at other conditions.

Determination of Axial Hot Gas Temperature Profile

The hot gas temperatures within the combustor were not measured directly but were taken to be equal to the wall temperatures measured with zero film cooling flow. With all film cooling flow shut off, the combustor was operated at a given set of conditions for a sufficient length of time for the test liner to be heated to a steady-state temperature. When no further change in test liner surface temperatures was observed, these temperatures were recorded as the baseline temperatures for subsequent liner cooling tests. This temperature profile closely approximates the axial hot gas temperature profile for hot stream Mach numbers less than 0.3, as encountered in typical subsonic combustion chambers. The following paragraph shows the reasoning.

When there is no further heat exchange between the hot gas stream and the liner, the adiabatic liner surface temperature at any downstream position x can be written as

$$T_{AW} = T_H \left(1 + r \frac{\gamma - 1}{2} M_H^2 \right)$$
(9a)

In equation (9a) $r = \sqrt[3]{Pr}$ is the temperature recovery factor for turbulent flow and $\mathscr{M}_H$ is the Mach number of the hot gas stream. Since at combustion chamber flow conditions $r \cong 0.9$ and $\gamma \cong 1.3$, equation (9a) can be written for these conditions as

$$T_{AW} = T_H\left(1 + 0.13\,\mathscr{M}_H^2\right) \tag{9b}$$

From equation (9b) it is easily seen that, for $\mathscr{M}_H < 0.3$, T_{AW} is only about 1 percent higher than T_H.

Thus, using the adiabatic liner test surface as a plate thermometer should be an acceptable method to determine the axial hot gas temperature profile in subsonic combustion chambers.

After the axial hot gas temperature profile was thus established, liner surface temperatures were measured with various mass rates of film cooling air blown over the test surface. For these tests care was taken to hold combustor exit temperature and reference velocity constant and at the values used to obtain the axial hot gas temperature profile. The film cooling air valves were then set at a desired flow rate and the liner surface and slot film temperatures were recorded after thermal equilibrium had been established. In this manner, liner surface temperature data were obtained for a range of film flow to hot flow ratios, with slot film temperature being determined by hot gas conditions and film flow rate.

Estimated Accuracy of Wall Temperatures

The wall temperature at each of the downstream stations used for subsequent data analysis was obtained by averaging the readings of the three thermocouples at each station.

The normal variation between these individual readings was approximately 50° F (28 K) with the maximum being 150° F (84 K) when a thermocouple was in the wake of a slot support, that is, in between two holes. Repeatability of thermocouple readings was within $\pm 25^\circ$ F (± 14 K). However, because of drift in combustor conditions and conduction errors in the test surface, the overall estimated error in the averaged surface temperature data is approximately $\pm 40^\circ$ F (± 22 K).

RESULTS AND DISCUSSION

In this section the liner wall temperature and slot pressure drop data will be discussed for the ten-slot configurations tested. Subsequently, the film cooling effective-

ness results will be compared to several correlations available in the literature and also to the turbulent mixing correlation proposed herein.

Wall Temperature Data

A complete listing of the raw wall temperature data is given in the appendix. The wall temperature profiles for the 0.3-inch (0.76-cm) slot are typical of the data obtained and are shown in figure 8 as a function of downstream distance from the slot denoted by x.
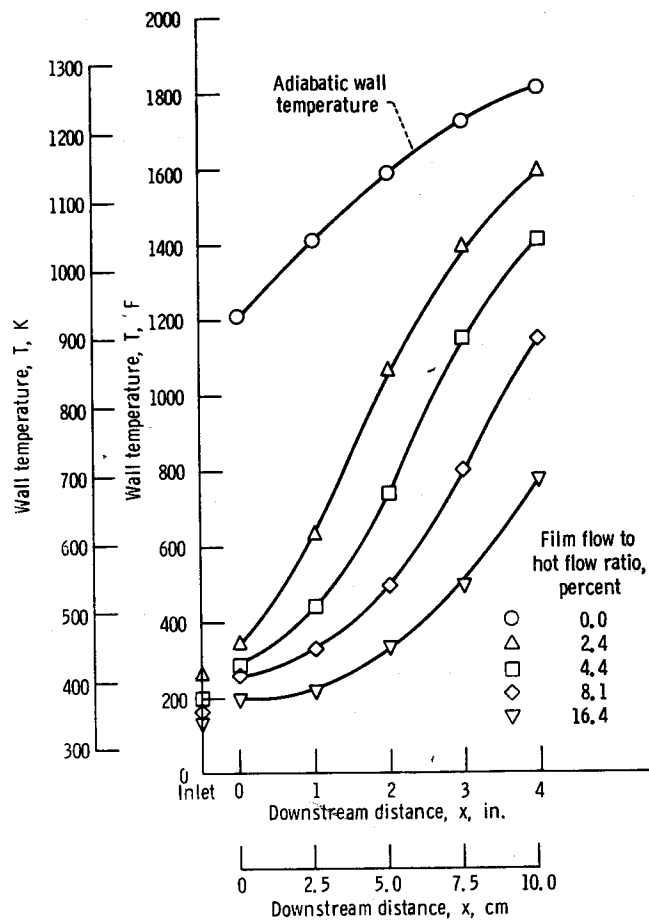
Figure 8. - Experimental wall temperature profiles for configuration 1 at various values of film flow to hot flow ratio. 0.3-Inch (0.76-cm) continuous slot; combustor exit temperature, 2000° F (1367 K); combustor reference velocity, 100 feet per second (30 m/sec).

At the station marked inlet, the cooling film temperatures at the slot are shown. Each of the temperature profiles shown in figure 8 represents a different film flow to hot flow ratio denoted by W_S/W_H. The top profile, obtained with zero film cooling flow, represents the adiabatic wall temperature which was previously shown to be practically equivalent to the axial hot gas temperature profile. The relatively steep slope of this profile is due to the combustion and mixing taking place in the region of the combustor chamber directly above the test surface.

Effect of Slot Geometry

Except for three of the configurations tested, the data for the slot geometries correlated well to the ratio of film to hot gas mass flow as shown in figure 9. Almost the
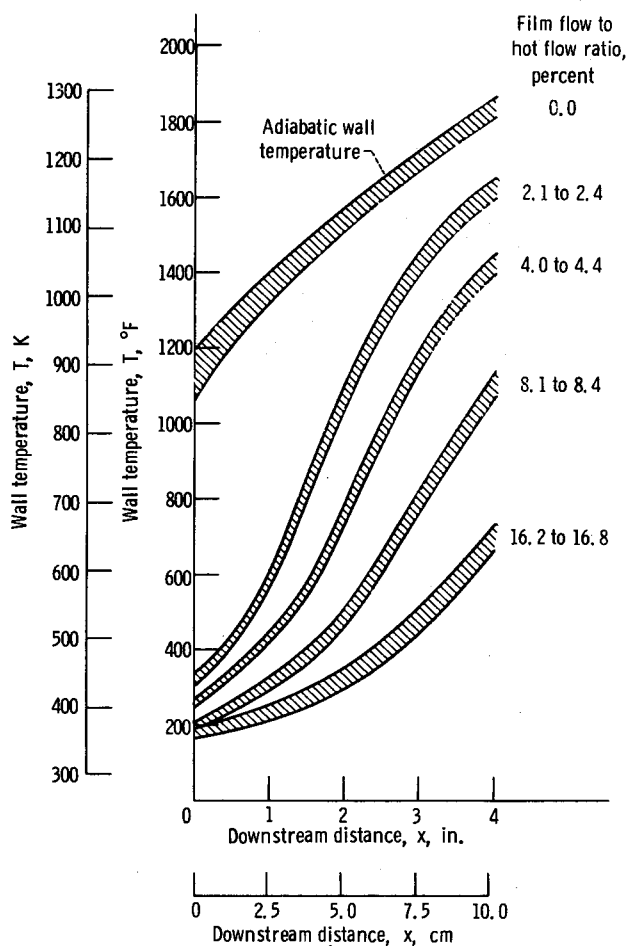
Figure 9. - Range of wall temperature profiles for configurations 1, 2, 4, 5, 6, 9, and 10 at various values of film flow to hot flow ratio. Combustor exit temperature, 2000° F (1367 K); combustor reference velocity, 100 feet per second (30 m/sec).

same wall temperatures were obtained at the same film mass flow rate as long as the flow behaved as a continuous sheet. In configurations such as metering holes angles at 45° to the slot the jets impinge on the upper slot lip and spread out before leaving the lip of the slot. In this way, the configuration behaves as a continuous slot.

For configurations 3, 7, and 8 (i.e., 0.0625-in. (0.16-cm) slot flush with the wall, 19 1/16-in. (0.16-cm) holes at 45°, and eight 3/16-in. (0.48-cm) holes at 0°, respectively) the film was less effective, and the wall temperatures increased faster than for the other configurations as shown in figure 10.

For configuration 3 (fig. 10(a)), the effect of the blocked slot area induced increased mixing between the film air and the hot stream. This detrimental effect of a thick slot lip was also reported by Kacker and Whitelaw in reference 8. When the blockage was
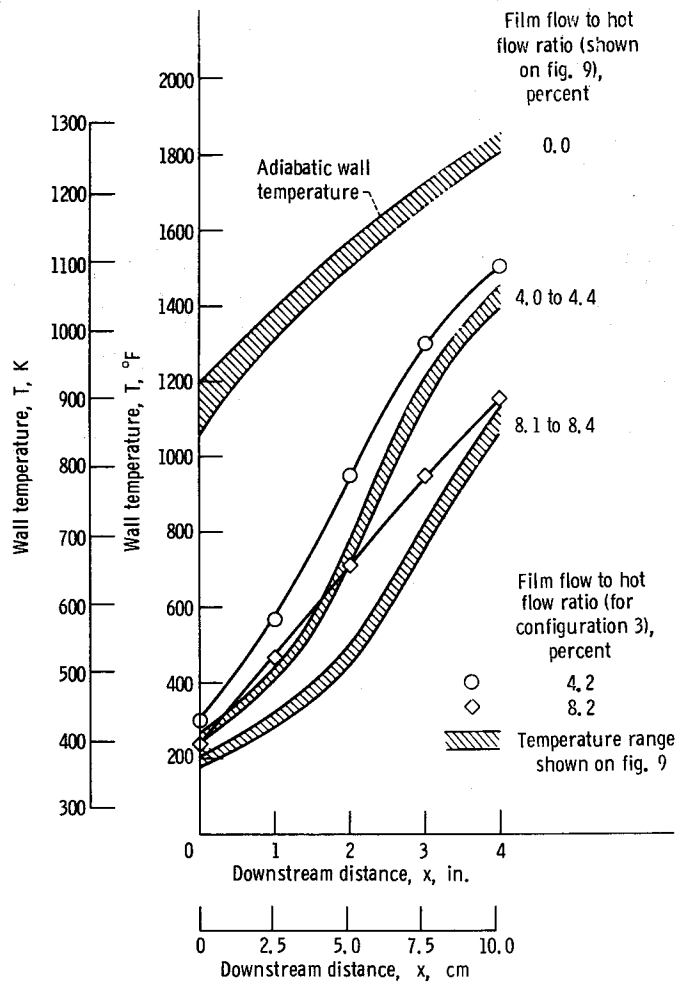
(a) Configuration 3: 0.0625-inch (0.16-cm) continuous slot flush with wall.

Figure 10. - Comparison of configurations 3, 7, and 8 with other configurations. Combustor exit temperature, 2000° F (1367 K); combustor reference velocity, 100 feet per second (30 m/sec).

21

(b) Configuration 7: 19 1/16-inch (0.16-cm) holes at 45°.

(c) Configuration 8: eight 3/16-inch (0.48-cm) holes at 0°.
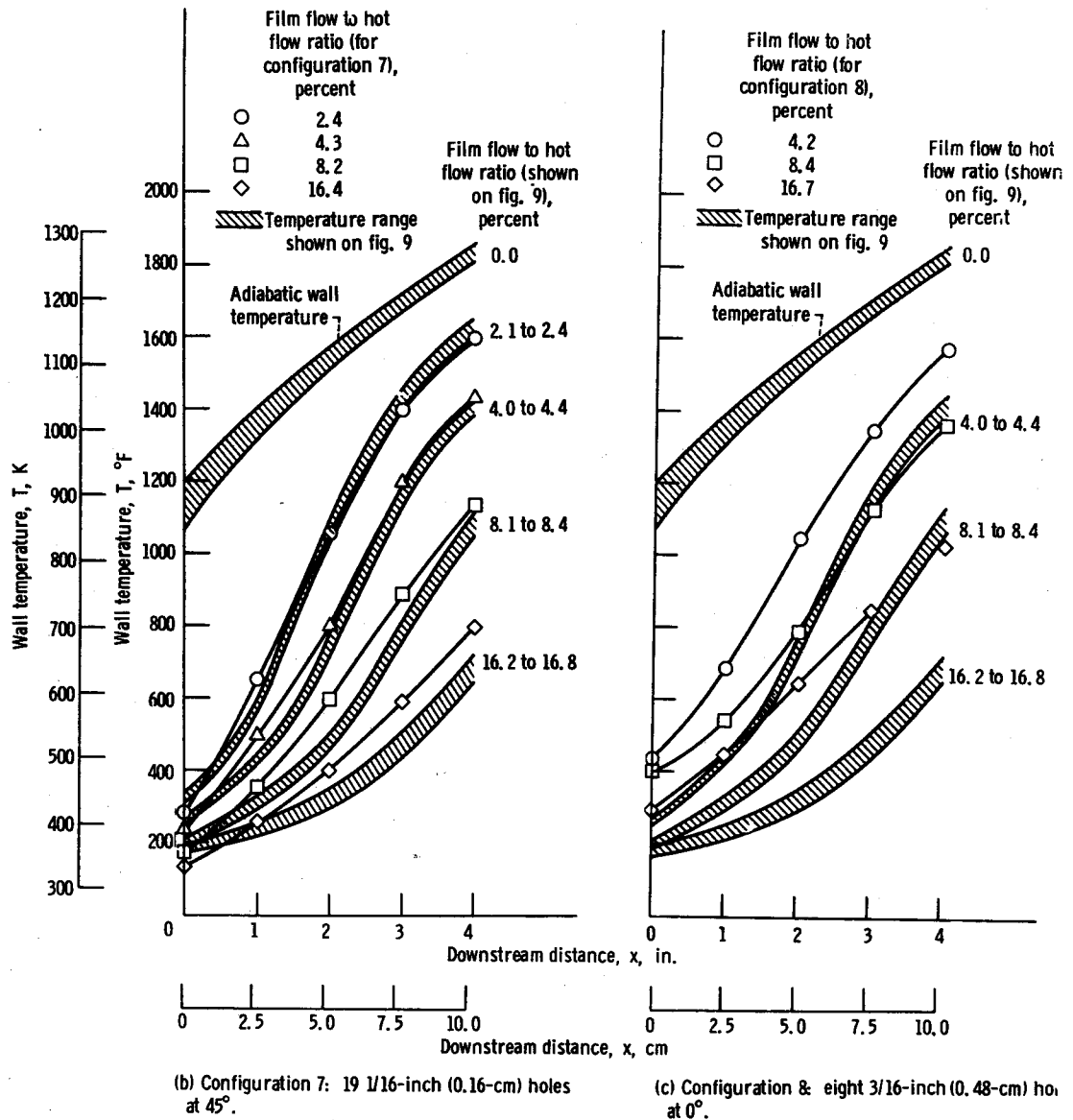
Figure 10. - Concluded.

placed below the slot (configuration 4), the wall temperatures were within the limits of the other configurations.

For configuration 7 (fig. 10(b)) the jet velocities at the holes were sonic for all but the lowest film flow. This jetting of the film air produced increased mixing between the hot main stream and the cooler jets.

For configuration 8 (fig. 10(c)) the jets did not form a continuous sheet as they left the slot. This allowed the hot gas to penetrate between the jets and resulted in increased temperatures for a given film cooling rate. This effect has also been noted by Metzger and Fletcher in reference 9. They showed that the wall temperatures for a series of

jets in a row were much higher than for a continuous slot even at the exits of the slots. This is the result of hot gas penetration as mentioned previously.

Effect of Changes in Mainstream Velocity and Temperatures

In order to detect any changes in data trends at other hot gas stream conditions, slot geometry 6 (four 1/4-in. (0.64-cm) holes) was also tested with a variation in combustor reference velocity and exit gas temperature. Figure 11(a) shows the surface tempera-
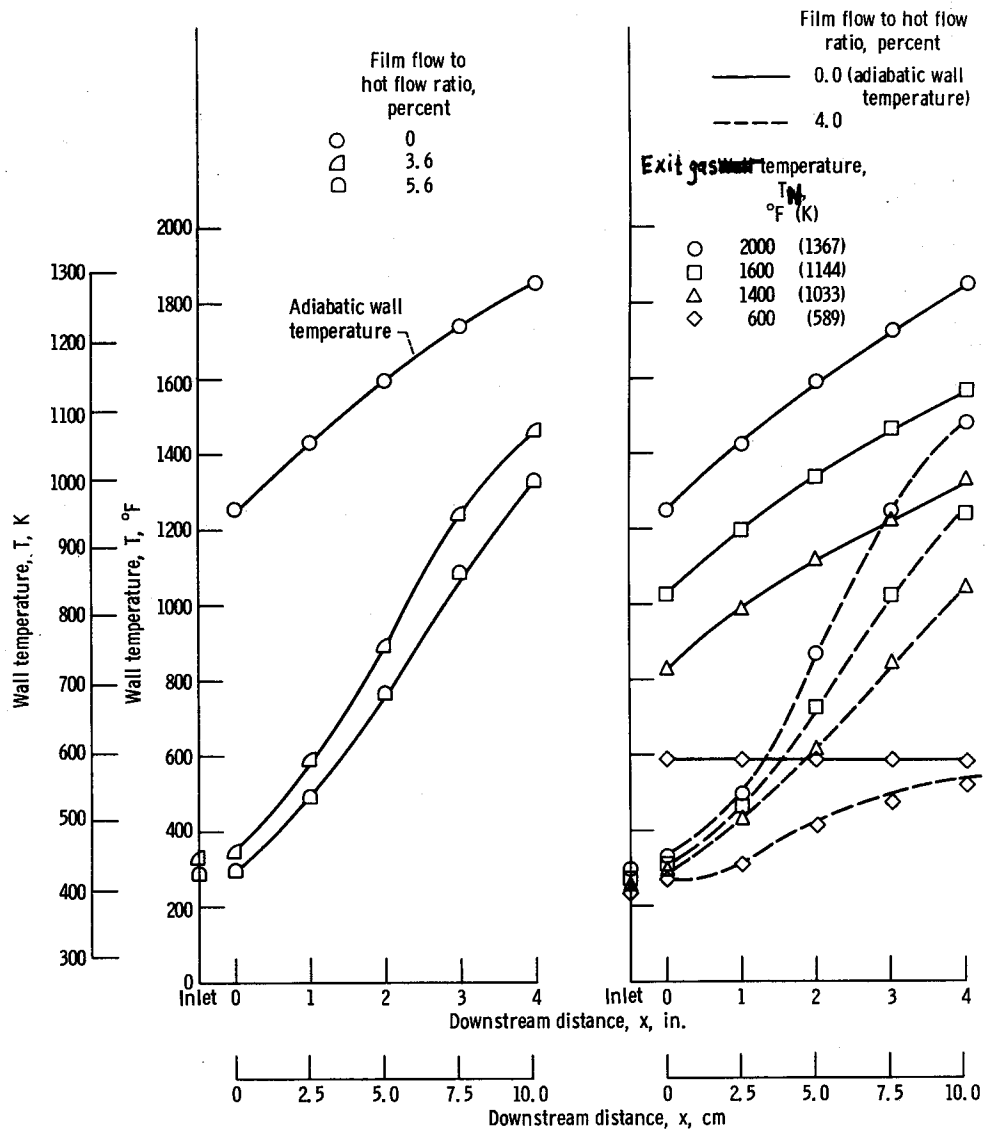
(a) Combustor reference velocity, 75 feet per second (23 m/sec); combustor exit temperature, 2000° F (1367 K).

(b) Combustor exit temperature varied from 600° to 2000° F (589 to 1367 K). Combustor reference velocity, 100 feet per second (30 m/sec); film flow to hot flow ratio, 0.0 and 4.0 percent.

Figure 11. - Effect of reference velocity and combustor exit temperature on wall temperature profiles for configuration 6: four 1/4-inch (0.64-cm) holes at 45°.

23

tures for two film flows obtained when the reference velocity was reduced to 75 feet per second (23 m/sec), with the exit temperature still at 2000° F (1367 K). The temperature profiles are comparable to those shown in figure 9 if changes in the mass flow ratic W_s/W_H are taken into account.

A parametric variation of exhaust gas temperature is shown in figure 11(b). The reference velocity was 100 feet per second (30 m/sec), and W_s/W_H was held at 4 percent. Adiabatic and film cooling wall data are shown for combustor exit temperatures of 600°, 1400°, 1600°, and 2000° F (589, 1033, 1144, and 1367 K). The wall temperatures are seen to follow the same pattern established previously, indicating that the film cooling mechanism is approximately the same for the hot stream conditions shown.

Several general observations can be made about the temperature profiles shown in figures 7 to 11; they are as follows:

(1) Wall temperature monotonically increases with downstream distance from the cooling slot for any W_s/W_H ratio.

(2) Wall temperatures always decrease whenever W_s/W_H is increased (i.e., an increase in film cooling flow reduces wall temperature and increases the film cooling effectiveness).

(3) Axial temperature profile variation due to changes in slot geometry is minor when film mass flow rate and inlet temperature are held constant.

(4) Configurations causing the flow to behave as a continuous film cooling sheet gave the best results. Configurations in this class were continuous slots and slots with hole centerlines at 45° to the liner test surface.

It should be pointed out that, although downstream liner temperatures were largely independent of slot geometry at constant film temperature and mass flow rate, the slot pressure drop required for a given amount of film flow was indeed determined by the slot geometry.

Slot Pressure Drop Data

Figure 12 shows the fractional pressure drop required to force a given mass flow through the various slot configurations. Some of the pressure drop values for the low area slot configurations are seen to be unrealistically high for practical application in combustors unless film flows are reduced to low values. Such low values of film flow, however, may be quite common with multiple slot liner geometries. Average pressure drop across liner cooling slots in state of the art combustion chambers is between 2 and 3 percent of combustor pressure. Thus the proper slot configuration would depend on the desired film cooling flow rate at the available pressure drop across the liner wall. The open continuous slots require a lower pressure drop to pass a given mass flow rate than the other configurations because of their larger flow area for a given total slot area.
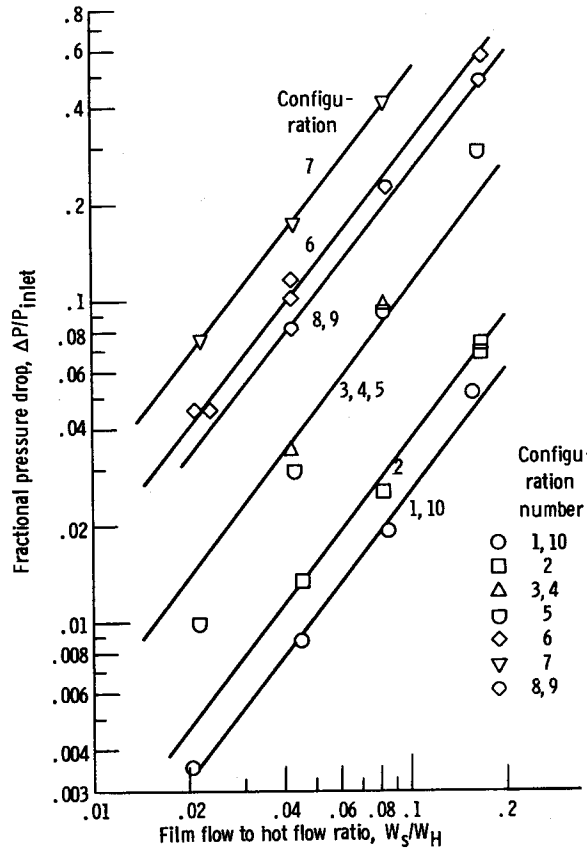
Figure 12. - Fractional pressure drop across slot as a function of film flow to hot flow ratio. Reference velocity, 100 feet per second (30 m/sec).

FILM COOLING CORRELATIONS

To obtain a direct comparison between the data of this report and correlations available in the literature, the wall temperatures were converted into film cooling effectiveness values in the following way:

$$\eta(x) = \frac{T_H(x) - T_W(x)}{T_H(x) - T_s}$$

(1)

In equation (1) the values η, T_H, and T_W are functions of the downstream distance x, while T_s is the temperature of the cooling film at the slot (i. e., at $x = 0$). Substituting into equation (1) the adiabatic wall temperature profiles obtained with zero film cooling flow for $T_H(x)$, the wall temperatures with film cooling for $T_W(x)$, and the temperature of the cooling film at the slot discharge for T_s, yield experimental film cooling effec-

25

TABLE II. - FILM COOLING CORRELATIONS

Correlation	Reference	Equation
Eckert and Birkebak (Wieghardt)	1	$$\eta = \dfrac{21.8}{\left(\dfrac{x}{Ms}\right)^{0.8}}$$
Stollery and El-Ehwany	2	$$\eta = \dfrac{3.09\left(Re_s\,\dfrac{\mu_s}{\mu_H}\right)^{0.2}}{\left(\dfrac{x}{Ms}\right)^{0.8}}$$
Hatch and Papell	3	$$\eta = \exp\left\{-\left[\left(\dfrac{hLx}{mC_p}\right)_s - 0.04\right]\left(\dfrac{sU_H}{\alpha}\right)^{0.125} f\left(\dfrac{U_H}{U_s}\right)\right\}$$ where $$f\left(\dfrac{U_H}{U_s}\right) = \begin{cases} 1 + 0.4\tan^{-1}\left(\dfrac{U_H}{U_s} - 1\right) & \text{for } U_H/U_s \geq 1 \\[2ex] \left(\dfrac{U_s}{U_H}\right)^{1.5\left[(U_s/U_H)-1\right]} & \text{for } U_H/U_s < 1 \end{cases}$$ and $$h = 0.0265\,\dfrac{k_f}{D_H}\,(Re_f)^{0.8}(Pr_f)^{0.3}$$
Spalding	4	$$\eta = \min\left(1.0,\ \dfrac{7}{X}\right)$$ where $$X = 0.91\left(\dfrac{U_H x}{U_s s}\right)^{0.8}(Re_s)^{-0.2} + 1.41\left(\dfrac{x}{s}\left|1 - \dfrac{U_H}{U_s}\right|\right)^{0.5}$$
NREC (modification of Spalding correlation)	11	$$\eta = \min\left(1.0,\ \left(\dfrac{3.5}{3.5\,X}\right)^{0.22},\ \dfrac{3.5}{X}\right)$$ where X is the same as in the Spalding correlation

TABLE II. - Concluded.   FILM COOLING CORRELATIONS

Correlation	Reference	Equation
Kutateladze and Leontev	5	$\eta = \dfrac{1}{\left(1 + 0.24\,Re_s^{-0.25}\,\dfrac{U_H}{U_s}\dfrac{x}{s}\right)^{0.8}}$
Carlson and Talmor	6	$\eta = \dfrac{1}{1 + 0.329\,aX_1}$ where $X_1 = \dfrac{Re_x^{0.8}}{Re_s}\dfrac{k_H}{k_s}\dfrac{Pr_H}{Pr_s}\left(\dfrac{P_e}{P_o}\right)^{(1/5)-\left\{\left[(1+m)/5\right]\left[(\gamma-1)/\gamma\right]\right\}}$ $\times \left(\dfrac{\sqrt{1 + \dfrac{\gamma-1}{2}\mathscr{M}_H^2}}{x\,\mathscr{M}_H^{27/7}} \displaystyle\int_0^x \dfrac{\mathscr{M}_H^{27/7}\,dx}{\sqrt{1 + \dfrac{\gamma-1}{2}\mathscr{M}_H^2}}\right)^{4/5}$
Turbulent mixing	---	$\eta = \dfrac{1}{1 + C_m\dfrac{x}{Ms}}$ where $C_m \cong \begin{cases} 0.03 \text{ to } 0.15 \text{ for combustors} \\[2ex] 0.01 \text{ for wind tunnels} \end{cases}$

tiveness values $\eta(x)$. It was previously pointed out that, for some slot configurations with holes, the film temperatures at the slot were higher than those for continuous slots. The reason was that the cooling gas thermocouples were located between wakes of jets issuing from holes. In this case the slot film temperature was taken to be equal to the average wall temperature at the $x = 0$ location. Cooling gas temperatures agreed within 90° F (50 K) or less with wall temperatures at the $x = 0$ location for all other slot configurations tested.

In an attempt to relate experimental film cooling effectiveness data to the known flow parameters, seven separate correlations were tried. These were the correlations proposed in references 1 to 6 and also the turbulent mixing model derived in the ANAL-YSIS section of this report. A listing of these correlations and the pertinent equations is given in table II.

In the following paragraphs the experimental film effectiveness data will be compared to each of the correlations. To aid in this comparison, plots of experimental film effectiveness values as functions of typical correlating parameters will also be presented for each of the correlations.

Eckert and Birkebak Correlation (Ref. 1)

The correlation presented in reference 1 was originally developed by Wieghardt (ref. 10) and is given by

$$\eta = \frac{21.8}{\left(\dfrac{x}{Ms}\right)^{0.8}} \tag{13}$$

Because of hot gas mass addition and combustor area change, the value of M was a decreasing function of x. Thus, in computing η from equation (13) the proper value of M for each station x was used. Shown in figure 13 is a plot of the experimental film effectiveness data as a function of the downstream distance parameter x/Ms. Also shown in this plot is the line of predicted effectiveness as given by equation (13). As shown by the narrow data scatter the experimental data of this report correlate remarkably well with the parameter x/Ms. However, the experimental η values decrease much more rapidly than values predicted by equation (13) as x/Ms increases. Thus, at x/Ms = 40, the experimental η are almost an order of magnitude lower than those calculated by equation (13).

The reason for this discrepancy is probably due to the difference between the flow
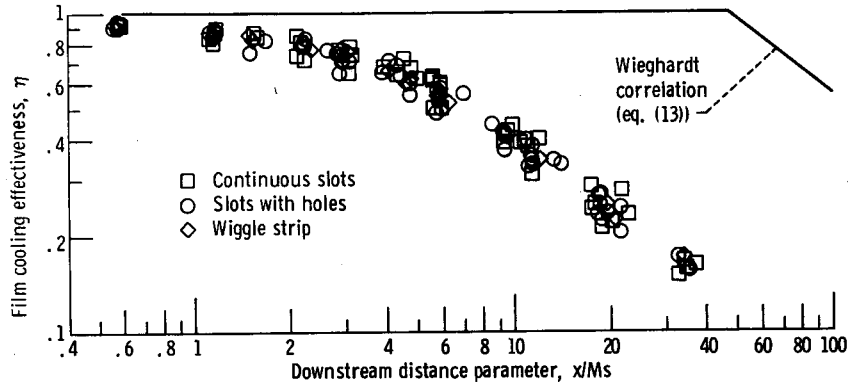
Figure 13. - Comparison of correlation used in reference 1 with experimental liner cooling data.

regime where equation (13) applies and the one under which the present data were obtained. The data reported herein were obtained in the highly turbulent mixing zone of a combustion chamber. Equation (13) on the other hand was developed on the basis of data obtained on airfoils suspended in a low turbulence wind tunnel. Hence, it is reasonable to assume that equation (13) would predict higher film cooling effectiveness values than could be obtained in the combustor tested.

Stollery and El-Ehwany Correlation (Ref. 2)

Using the concept of a developing boundary layer, Stollery and El-Ehwany apply a slot Reynolds number and viscosity correction to the Wieghardt correlation shown in equation (13). Their correlation is given by

$$\eta = \frac{3.09\left(Re_s \frac{\mu_s}{\mu_H}\right)^{0.2}}{\left(\frac{x}{Ms}\right)^{0.8}} \tag{14}$$

The effect of slot Reynolds number accounts for the slot induced turbulence. When the mainstream turbulence is low, this factor usually reduces the scatter in the data. However, in the present work the effect of slot induced turbulence was small.

By including the effect of slot Reynolds number, the scatter in the experimental data is actually increased slightly as shown in figure 14. Yet the scatter is still low, maxi-

29
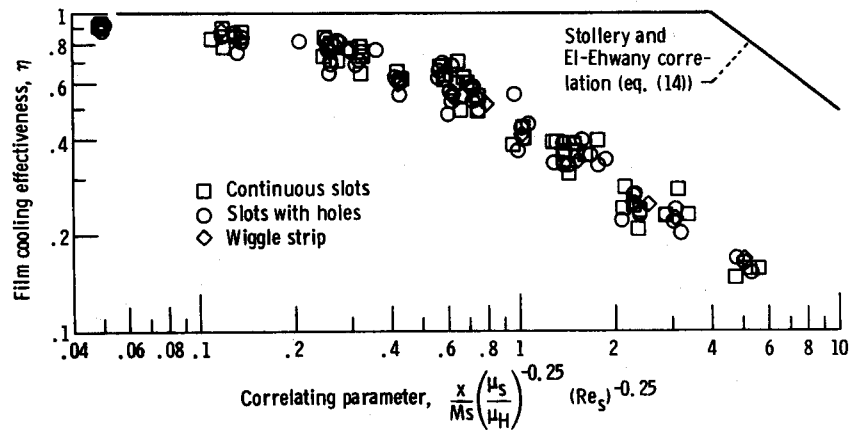
Figure 14. – Comparison of Stollery and El-Ehwany correlation with experimental liner cooling data.

mum deviations being approximately ±25 percent of mean effectiveness values at any abscissa value.

Again it should be noted that the experimental data decrease more rapidly, as the abscissa term increases, than the line representing equation (14). The reason for this appears to be the same as cited previously for equation (13).

Hatch and Papell Correlation (Ref. 3)

This correlation, given by

$$\eta = \exp\left\{-\left[\frac{hLx}{\left(mC_p\right)_s} - 0.04\right]\left(\frac{sU_H}{\alpha}\right)^{0.125} f\left(\frac{U_H}{U_s}\right)\right\} \tag{15}$$

where

$$f\left(\frac{U_H}{U_s}\right) = \begin{cases} 1 + 0.4 \tan^{-1}\left(\frac{U_H}{U_s} - 1\right) & \text{for } U_H/U_s \geq 1 \\ \left(\frac{U_s}{U_H}\right)^{1.5\left[(U_s/U_H)-1\right]} & \text{for } U_H/U_s \leq 1 \end{cases}$$

considers forced convection heat transfer between the main gas stream and the film and

30
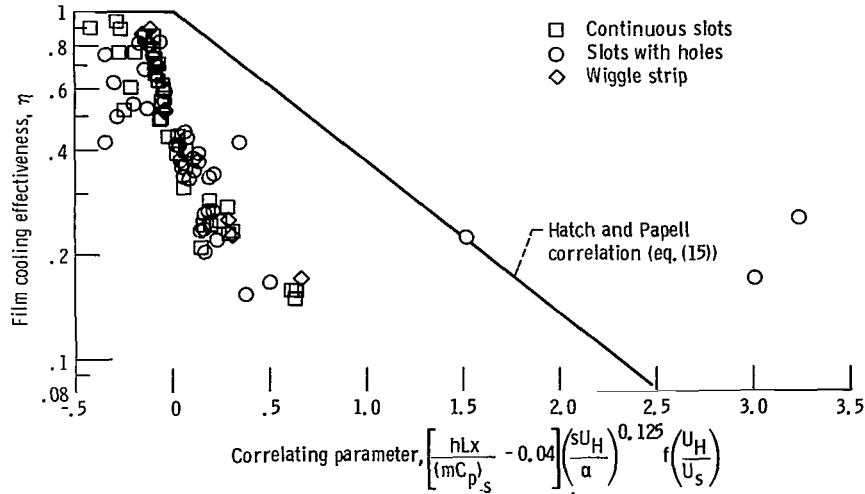
Figure 15. - Comparison of Hatch and Papell correlation with experimental liner cooling data.

contains an empirical correction for the hot gas to film velocity ratio. The film cooling effectiveness data are plotted in figure 15. For purposes of comparison with the previous correlations, the term in brackets can be rearranged using the appropriate correlation for the convective coefficient to obtain a form similar to the previous correlations. This term then becomes

$$\left[\frac{hxL}{\left(mC_p\right)_s} - 0.04\right] = \left[\frac{hx}{\left(\rho UC_p\right)_s} - 0.04\right]$$

$$= \left[0.0265\left(\frac{x}{Ms}\right)\left(\frac{C_{p_H}}{C_{p_S}}\right)(Re_H)^{-0.2}(Pr_H)^{-0.7} - 0.04\right] \tag{16}$$

From equations (16) and (15) it can be seen that this correlation takes into account the x/Ms ratio, the ratio of heat capacities of the two streams, the Reynolds and Prandtl numbers of the mainstream, and the ratio of hot gas to film velocity. The last of these effects is taken into account by the function $f(U_H/U_s)$.

A negative value for the term in brackets in equation (15) would result in a film cooling effectiveness greater than 1.0 which is physically impossible. Therefore, for these conditions, the film cooling effectiveness is automatically set equal to 1.0. For the data obtained herein, the velocity ratio function ranged from approximately unity for

31

$U_H/U_S \geq 1.0$ to as high as 10^8 for $U_H/U_S \leq 0.15$. Substituting such high multiplicative terms into the correlation (eq. (15)) will yield η values of practically zero. Thus, the correlation overestimated the film cooling effectiveness whenever the value of the term in brackets (see eq. (15)) was negative ($\eta_{calc} = 1.0$) and also when the term in brackets was positive coupled with low $f(U_H/U_S)$ values ($\eta_{calc} \cong 0.6$ to 1.0). Conversely, it underestimated η at positive bracket values coupled with high values for $f(U_H/U_S)$ and ($\eta_{calc} = 0$). Figure 15 shows experimental values to be generally lower than those predicted by a factor of 1.5 to 4, and a high degree of scatter is present. This is because the correlation overestimated the effect of the relative velocity. Furthermore, the high turbulence level in the test combustor may explain why the experimental effectiveness data fall below the line predicted by the correlation. As indicated previously, high turbulence has an adverse effect on film effectiveness.

Spalding Correlation and NREC Modification (Refs. 4 and 11)

These correlations are based on a parameter proposed by Spalding, which has the form

$$X = 0.91\left(\frac{U_H}{U_S}\frac{x}{s}\right)^{0.8}(Re_S)^{-0.2} + 1.41\left(\frac{x}{s}\left|1 - \frac{U_H}{U_S}\right|\right)^{0.5} \tag{17}$$

Using X as the correlating parameter, Spalding suggests that the film cooling effectiveness be computed from the function

$$\eta = \min\left(1.0, \frac{7}{X}\right) \tag{18}$$

Since equation (18) predicts η values that tend to be too optimistic for combustor liners, NREC proposes that the expression for film cooling effectiveness be modified to

$$\eta = \min\left(1.0, \left(\frac{3.5}{3.5\,X}\right)^{0.22}, \frac{3.5}{X}\right) \tag{19}$$

Figure 16(a) shows the experimental film effectiveness data plotted as a function of the parameter X. Also shown on this plot are the lines representing equations (18) and (19). Note that the NREC modification (eq. (19)) is more in line with the lower η values obtained herein.

32

Correlating parameter, $X = 0.91\left(\dfrac{U_M}{U_S}\dfrac{x}{s}\right)^{0.8} Re^{-0.2} + 1.41\left(\dfrac{x}{s}\left|1-\dfrac{U_H}{U_S}\right|\right)^{0.5}$
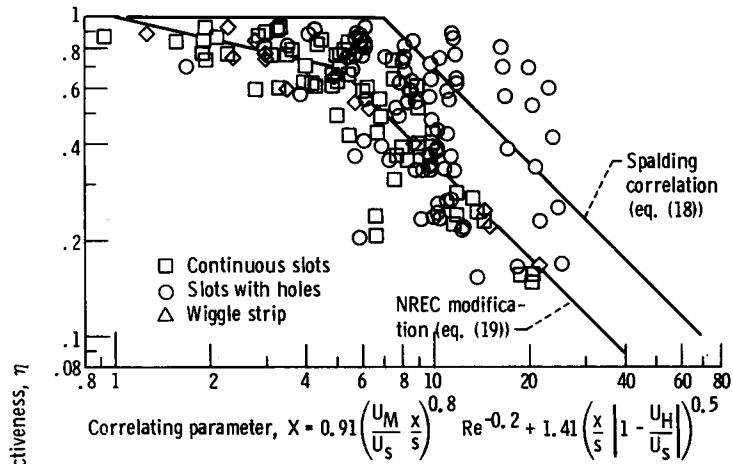
(a) Comparison of Spalding correlation and NREC modification of Spalding correlation with experimental liner cooling data.
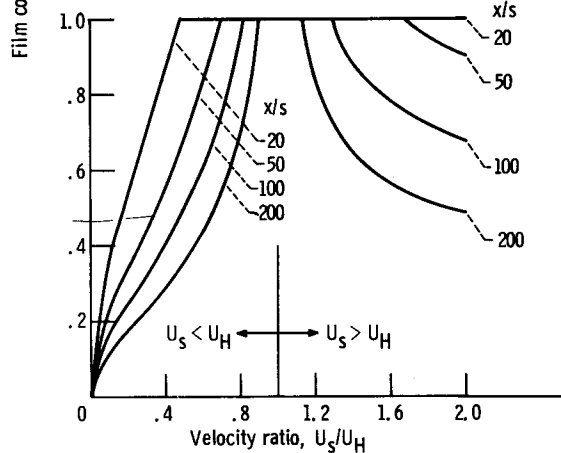
(b) Effect of velocity ratio on film cooling effectiveness using Spalding correlation. Slot height, 0.3 inch (0.76 cm); cooling air temperature, 60° F (289 K); hot gas velocity, 400 feet per second (120 m/sec).

Figure 16. - Evaluation of Spalding's parameter X for film cooling data.

The high degree of data scatter is due to the fact that the mass flux ratio of the film to hot stream is not taken into account by the correlating parameter. Equation (17) shows that this parameter is essentially the sum of a velocity ratio term and a term expressing the relative velocity between the film and the hot stream. Since the relative velocity term predominates (its value was found to be 3 to 20 times higher than the value for the first term for the data of this study), in most cases the predicted value of η was found to decrease as the absolute value of relative velocity $|U_H - U_S|$ is increased. The correlation hence predicts an increase in film cooling effectiveness when slot velocity U_S is increased as long as the slot velocity is less than the hot gas velocity

33

(i.e., $U_S < U_H$). This is in agreement with experimental data trends. However, if U_S is increased under the condition that $U_S > U_H$ (i.e., the slot velocity is greater than the hot gas velocity), the computed value of η will actually decrease at high enough x/s values. This is contrary to data trends. Figure 16(b) illustrates the effect of U_S/U_H on the computed effectiveness η for a 0.3-inch (0.76-cm) slot at the conditions indicated on the figure. The curves drawn for various x/s ratios show that η, as computed by equation (18), decreases for $U_S/U_H > 1$ and $x/s > 50$.

A conclusion that can be drawn is that, for the data considered, induced turbulence due to differences in velocity between the hot gas stream and the film had a much smaller effect on η than the mass flux ratio $M = \rho_S U_S / \rho_H U_H$. Unfortunately, density ratio, which when multiplied by U_S/U_H does yield M, does not appear in equation (17).

A possible reason for the apparent insensitivity of the data to relative velocity between the film and the hot stream is that the mixing due to velocity difference is small when compared to the mixing caused by the high mainstream turbulence. This was also suggested by Sturgess (ref. 12) who used the Spalding correlation to reduce combustor data and found that it overestimated film cooling effectiveness.

Kutateladze and Leontev Correlation (Ref. 5)

This correlation is given by the expression

$$\eta = \frac{1}{\left(1 + 0.24 \, Re_s^{-0.25} \, \dfrac{U_H}{U_S} \dfrac{x}{s}\right)^{0.8}} \tag{20}$$

Equation (20) was derived with the assumption of a turbulent film and a nonaccelerating hot gas flow, with the gas properties being constant.

The experimental data and the correlation are shown in figure 17. With the exception of a few data points, the scatter is within acceptable limits. The points falling outside the data band represent test conditions where the hot gas to film density ratio deviated significantly from the mean density ratio for the other data points. Had the density ratio been included in the correlating parameters, the few stray data points would also have fallen inside the band. Thus, the need for including the mass flux ratio M rather than just the velocity ratio U_H/U_S in the correlating parameter is again demonstrated. The correlation predicts effectiveness values up to twice as high as was obtained experimentally. Again, as suggested in connection with previously discussed correlations, this appears to be due to the combustor hot gas stream turbulence.

34
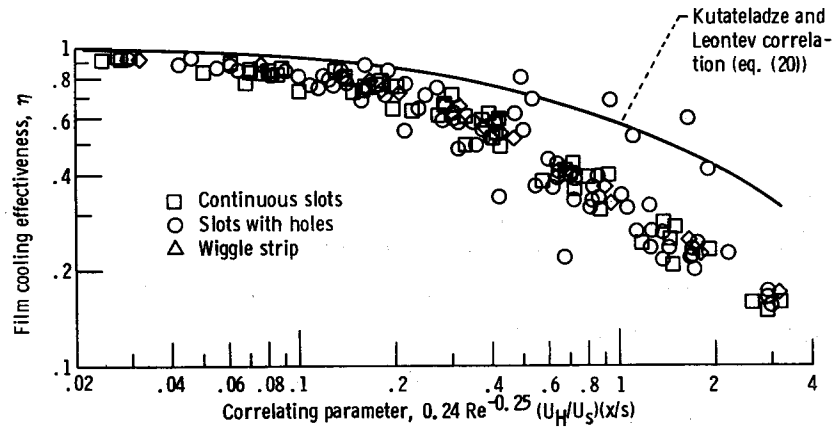
Figure 17. - Comparison of Kutateladze and Leontev correlation with experimental liner cooling data.

Carlson and Talmor Correlation (Ref. 6)

The correlation of Carlson and Talmor is given by

$$\eta = \frac{1}{1 + 0.329 \, aX_1} \tag{21}$$

where

$$X_1 = \frac{Re_x^{0.8}}{Re_s} \frac{k_H}{k_s} \frac{Pr_H}{Pr_s} \left(\frac{P_e}{P_o}\right)^{(1/5) - \left\{\left[(1+m)/5\right]\left[(\gamma-1)/\gamma\right]\right\}}$$

$$\times \left(\frac{\sqrt{1 + \frac{\gamma - 1}{2} \mathcal{M}_H^2}}{x \mathcal{M}_H^{27/7}} \int_0^x \frac{\mathcal{M}_H^{27/7} \, dx}{\sqrt{1 + \frac{\gamma - 1}{2} \mathcal{M}_H^2}}\right)^{4/5} \tag{22}$$

The correlation was derived by assuming that the boundary layer grows as a fully developed isothermal boundary layer on a flat plate and a one-seventh power velocity profile. The effect of turbulence is introduced into equation (21) through the mixing coefficient a. The mixing coefficient increases with increasing turbulence levels and increasing rate of hot gas acceleration.

Carlson and Talmor determined the relation between a and turbulence level as fol-

35

lows. The magnitude of a was determined experimentally by comparing film cooling data with equation (21). Turbulence was produced by using various sized grids, and the magnitude of the turbulence level was calculated at the slot exit. For a turbulence intensity of 3.2 percent, a was found to equal 1; at a turbulence level of 22 percent, a = 3. These values of the mixing coefficient a were obtained with no hot gas acceleration. The calculated turbulence decreased over the test section from a value of 3.2 percent at the slot exit to 1.14 percent at the end of the test section for the low turbulence grid, and from a value of 22 percent to a value of 8 percent for the high turbulence grid.

The correlation does not adequately account for hot gas acceleration so that the mixing coefficient must be varied as the hot gas acceleration increases. A value of the mixing coefficient as high as 12 is required at a turbulence level of 10 percent and a wall angle of 60°. The mixing coefficient a also had to be a function of downstream distance in order to obtain agreement with their experimental data. Carlson and Talmor do not suggest a relation for the variation of the mixing coefficient with turbulence and hot gas acceleration. They suggest only the values given previously for the effect of turbulence without hot gas acceleration.

The experimental data of this report are plotted in figure 18 as a function of the parameter X_1. A value of a as high as eight is needed to obtain agreement with the data. It is not possible to compare this value with a predicted value since Carlson and Talmor do not combine the effects of hot gas acceleration and turbulence into a single equation for determining a.

$$X_1 = \frac{Re_x^{0.8}}{Re_s} \frac{k_H}{k_s} \frac{Pr_H}{Pr_s} \left(\frac{P_e}{P_0}\right)^{(1/5)-\{(2.5/5)[(\gamma-1)/\gamma]\}} \left(\frac{\sqrt{1+\frac{\gamma-1}{2}\mathcal{M}_H^2}}{x\mathcal{M}_H^{27/7}} \int_0^x \frac{\mathcal{M}_H^{27/7}dx}{\sqrt{1+\frac{\gamma-1}{2}\mathcal{M}_H^2}}\right)^{4/5}$$
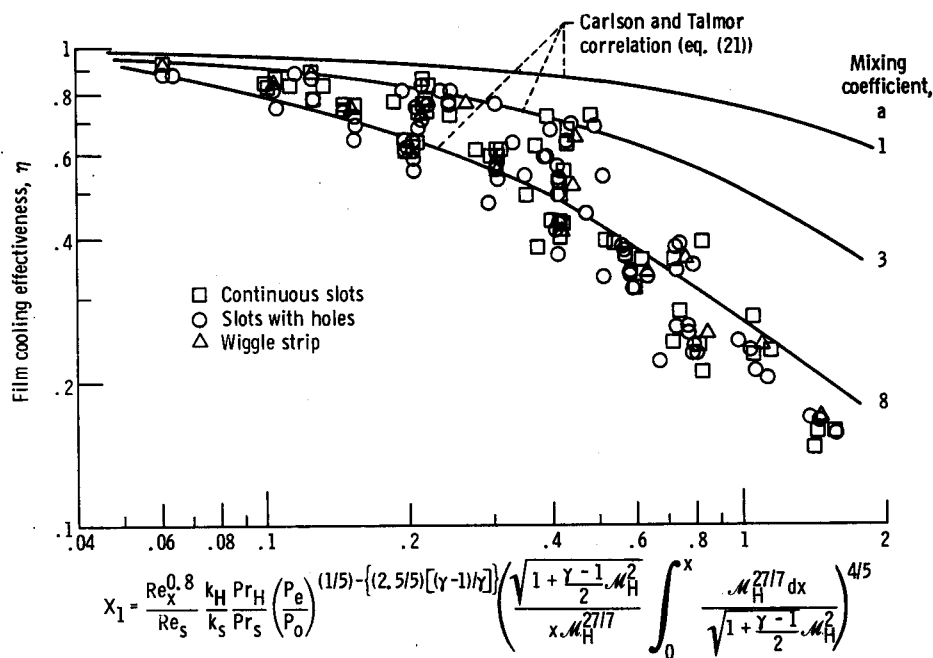
Figure 18. – Comparison of Carlson and Talmor correlation with experimental liner cooling data.

Instead, they leave the constant a to be based strictly on empirical results. The correlation shows considerable scatter with a maximum deviation of 60 percent for a value of a = 8.

Turbulent Mixing Correlation

In an attempt to take into account the turbulence level of the hot gas stream, a simple one-dimensional mass mixing model was derived as shown in the ANALYSIS section of this report. The expression for film effectiveness for the case where the hot gas and the film are of the same composition was shown to be

$$\eta = \frac{1}{1 + C_m \frac{x}{Ms}} \tag{7}$$

Although equation (7) was derived with the assumptions of constant hot gas temperature T_H and mass flux ratio M, it was still able to correlate combustor data as long as the correct values of $T_H = T_H(x)$ and $M = M(x)$ were used at each measuring station downstream from the slot x.

In this model the mixing rate between the mainstream and the film is assumed to be a function of turbulence level which must be estimated for a given application. The resulting flexibility of this model was illustrated in figure 2 where maps of η as a function of x/Ms curves are generated for a wide and a narrow range of abscissa values, respectively, by letting the turbulent mixing level C_m vary from 0.005 to 0.20. These maps are typical of film cooling data trends published in the literature (refs. 1 to 6). For the data of this report, the value of C_m was assumed to be 0.15 in order to obtain the data fit illustrated in figure 19. This figure shows the ±20 percent agreement be-
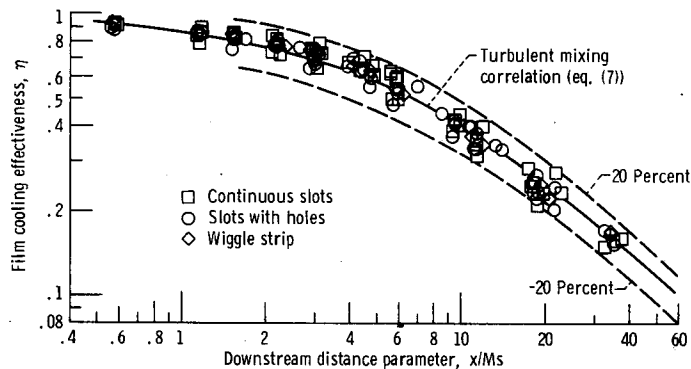
Figure 19. - Comparison of turbulent mixing correlation (C_m = 0.15) with experimental liner cooling data.

tween experimental and predicted values for all the slot geometries considered herein.

If the additional assumption of a one-to-one correspondence between turbulent mixing level C_m and turbulence level τ is made, the assumed value of $C_m = 0.15$ does agree with estimated values of combustion chamber turbulence level. From cold flow hot wire measurements these values of τ were found to range from 10 to 20 percent for the combustor tested, with 15 percent representing an average value.

Figure 20 is a plot of the actual wall temperature error obtained by comparing the temperatures predicted by the model to experimental measurements. This error is seen to be less than $\pm 100^{\circ}$ F (± 55 K) for practically all of the data shown. These data represent the lower temperatures of the $x = 1$ inch (2.5 cm) station as well as the high wall temperatures of the downstream station at $x = 4$ inches (10 cm). Intermediate data (i.e., at the $x = 2$ in. (5 cm) and $x = 3$ in. (7.5 cm) stations) also were within the above error limits. These data were omitted from the plot in the interest of clarity.
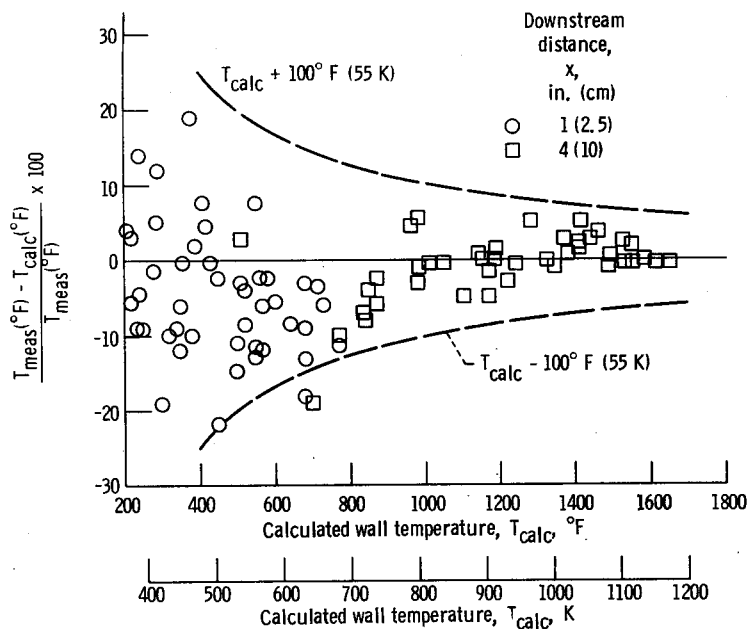
Figure 20. - Error in predicted wall temperature using turbulent mixing correlation ($C_m = 0.15$).

To test the turbulent mixing model at conditions of low turbulence level, the model was applied to the data of reference 1. The assumed value of turbulence level was 1 percent, as given by Schlichting (ref. 13) for typical wind tunnels. Figure 21 shows the good agreement with the data (approximately ± 15 percent) obtained throughout the range of x/Ms, including the lower values where the straight line correlation, (eq. (13)) predicts η values of unity.

38
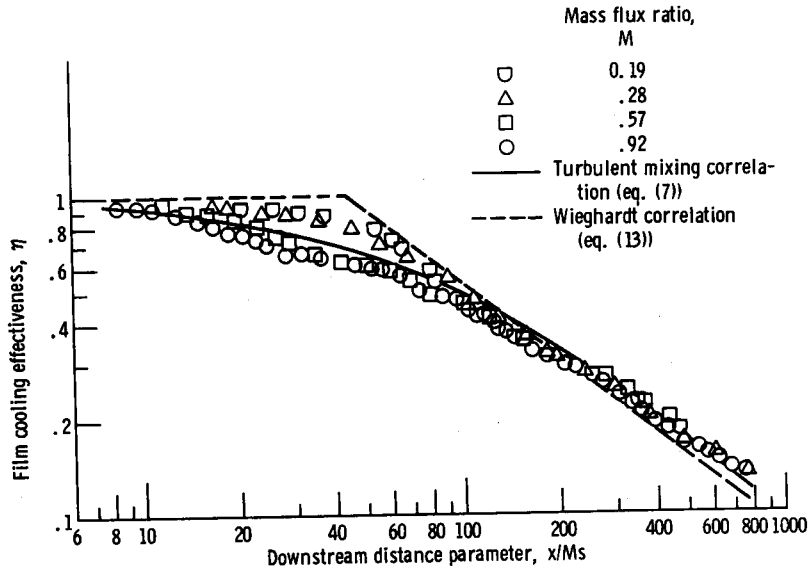
Figure 21. - Turbulent mixing correlation (C_m = 0.01) and Wieghardt correlation applied to data of Eckert and Birkeback.

The helium cooling data of Hatch and Papell (ref. 3) were also used to test the mixing equation which was modified to include the effect of the heat capacity differences as shown in equation (8) which is repeated here

$$\eta = \cfrac{1}{1 + C_m \cfrac{x}{Ms} \cfrac{C_{p_H}}{C_{p_S}}} \tag{8}$$

The data for three slot heights are plotted in figure 22 for the hot gas temperatures and velocity ratios shown. Coolant temperatures ranged from 45° F (280 K) for the highest velocity ratio to 560° F (544 K) for the lowest velocity ratio.

As shown in these figures the turbulent mixing model (eq. (8)) correlates the data for the 0.125-inch (0.31-cm) slot quite well with an assumed C_m = 0.01 (fig. 22(a)).

As the slot height is increased (figs. 22(b), (c). and (d)), the experimental data approach the C_m = 0.02 line at abscissa values greater than 50. This could be due to the increased slot induced turbulence which, contrary to observations in combustors, does have a significant effect on the film cooling effectiveness of low turbulence ducts. The data points falling above the C_m = 0.01 line at high abscissa values represent measurements made for low film flow velocities as far as 34 inches (86 cm) from the slot. It is assumed that, at this distance, the film had become completely mixed with the hot gas stream and wall surface temperatures were no longer increasing. Even so about 90 per-
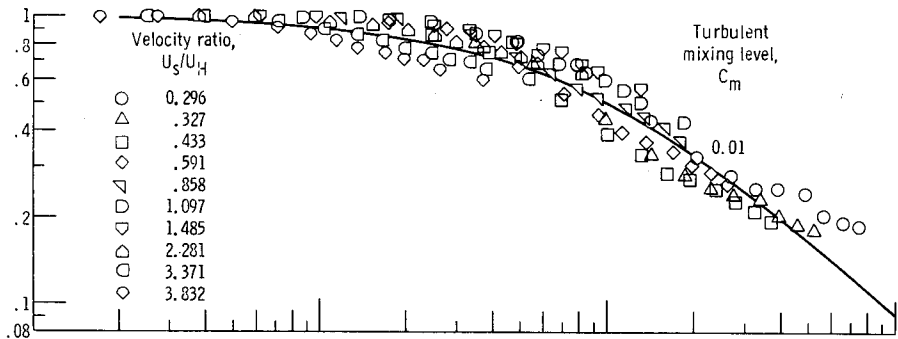
(a) Equivalent slot height s = 0.125 inch (0.31 cm); hot gas temperature T_H = 1015° F (819 K).
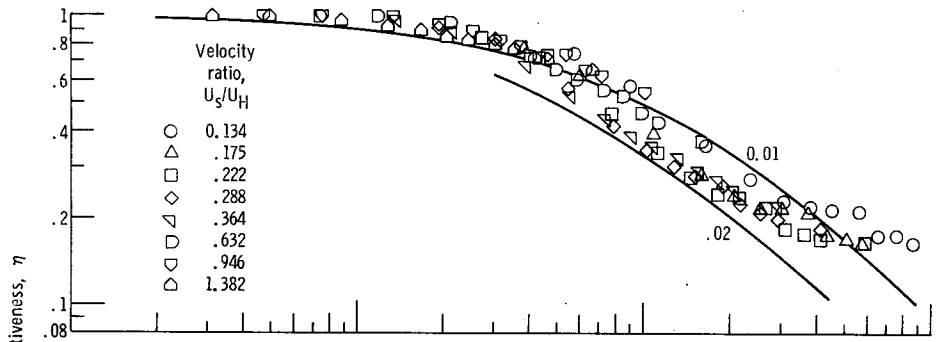
(b) Equivalent slot height s = 0.25 inch (0.62 cm); hot gas temperature T_H = 1015° F (819 K).
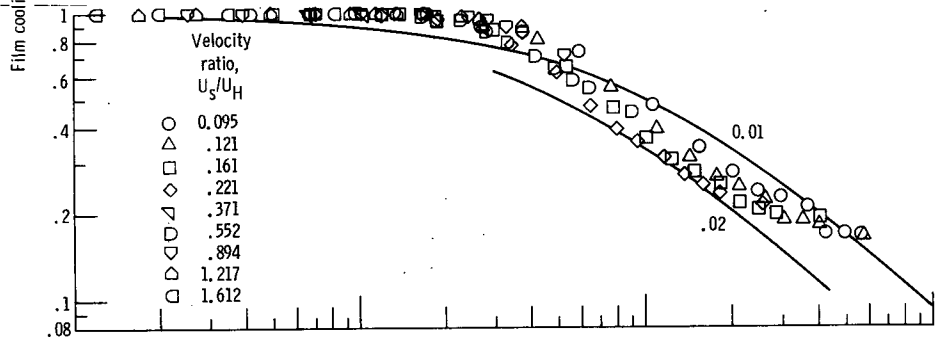
(c) Equivalent slot height s = 0.50 inch (1.27 cm); hot gas temperature T_H = 1015° F (819 K).
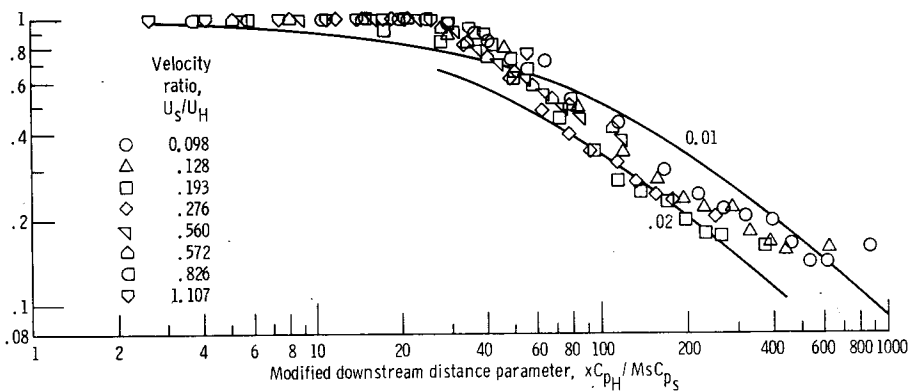
(d) Equivalent slot height s = 0.50 inch (1.27 cm); hot gas temperature T_H = 540° F (556 K).

Figure 22. - Turbulent mixing correlation applied to helium coolant data of Hatch and Papell.

cent of the film effectiveness data obtained in reference 3 could be correlated within ±30 percent by equation (8), with $C_m = 0.01$. The corresponding wall surface temperature errors were within ±100° F (±55 K).

SUMMARY OF RESULTS

Film cooling effectiveness data for various slot geometries were obtained using an instrumented liner installed in a rectangular sector of a gas turbine combustor. On the basis of these data, a simple turbulent mixing model was developed.

The following results were obtained:

1. The turbulent mixing model described in this report predicted film cooling effectiveness values for the liner tested within ±20 percent.

2. Actual surface temperatures were predicted within approximately ±100° F (±55 K) or less.

3. The model correlated all of the film cooling effectiveness data of Eckert and Birkebak within ±15 percent. It also correlated about 90 percent of the film cooling effectiveness data of Hatch and Papell within ±30 percent.

4. The effect of slot geometry on film cooling effectiveness is small at a given cooling mass flow rate.

5. In general, continuous slots and slots with holes at 45° produced the lower surface temperatures for each cooling mass flow rate. For these slots the cooling film acted as a continuous sheet.

6. Somewhat higher surface temperatures were obtained with slot configurations 3, 7, and 8. For these slots increased mixing occurred between the film and the hot gas stream. For configuration 8 initial hot gas penetration between the cooling jets also increased the cooling film temperature at the slot.

CONCLUDING REMARKS

The simple turbulent mixing model should be able to predict film cooling effectiveness values for combustors and other environments if the approximate turbulence level or turbulence level variation with downstream distance can be estimated. If slot turbulence or the turbulence generated by large velocity differences is high, relative to the turbulence level in the duct, then these additional parameters may need to be taken into account to obtain good accuracy. If mass is being added to the hot stream in the region where liner surface temperatures are to be determined, the mass flux ratio M should be allowed to vary with downstream distance from the slot. Also the axial hot gas tem-

perature profile must be estimated. This might be done by considering the cumulative fraction of fuel burnt at different downstream stations and using the ideal combustion temperature. If this is not possible, the highest hot gas temperature can be used. The predicted values of wall temperature will be higher than actual in this case.

Several advantages of the model are the following:

1. It can correlate data from widely different flow regimes if the turbulent mixing level can be measured or estimated.

2. The variation of film cooling effectiveness with turbulent mixing level can readily be estimated from the correlation.

3. It is simple to apply; the only input values necessary are effective slot height s, mass flux ratio M, downstream distance x, and turbulent mixing level C_m.

Lewis Research Center,
    National Aeronautics and Space Administration,
        Cleveland, Ohio, February 23, 1971,
           720-03.

APPENDIX - COMBUSTOR FILM COOLING DATA

The test stand data used to calculate film cooling effectiveness for the various slot configurations are listed in table III. Measurements were made in U. S. customary units and converted to SI units.

TABLE III. - LINER FILM COOLING DATA

(a) U. S. Customary units

Run	Mass flow rate of hot stream, lb/sec	Combustor exit temperature, °F	Mass flow rate of cooling air, lb/sec	Slot velocity, ft/sec	Mass flux ratio at x = 1 in.	Inlet cooling air temperature, °F	Wall temperature, °F, at specified downstream distances in inches			
							1.0	2.0	3.0	4.0
Configuration 1: 0.3-inch (0.76-cm) continuous slot							Axial hot gas temperature profile, °F			
1	4.00	1800	0.0	0.0	0.0	---	980	1250	1415	1510
2	4.00	1800	0.159	304	5.6	140	215	325	470	665
3	4.00	1800	.085	173	3.0	180	310	425	660	1000
4	4.00	1800	.045	99	1.6	230	430	745	950	1200
5	4.00	1800	.022	55	.8	330	570	920	1120	1325
Configuration 1: 0.3-inch (0.76-cm) continuous slot							Axial hot gas temperature profile, °F			
6	4.00	2000	0.0	0.0	0.0	---	1410	1590	1715	1810
7	4.00	2000	0.024	54	0.8	255	635	1070	1380	1580
8	4.00	2000	.044	93	1.6	200	440	750	1150	1410
9	4.00	2000	.081	161	2.9	165	330	500	800	1150
10	4.00	2000	.164	310	5.8	134	215	320	500	780
Configuration 2: 0.156-inch (0.4-cm) continuous slot							Axial hot gas temperature profile, °F			
11	4.00	1800	0.0	0.0	0.0	---	1140	1340	1470	1550
12	4.00	1800	0.165	591	11.5	110	180	300	430	600
13	4.00	1800	.081	310	5.6	150	250	400	680	950
Configuration 2: 0.156-inch (0.4-cm) continuous slot							Axial hot gas temperature profile, °F			
14	4.00	2000	0.0	0.0	0.0	---	1280	1510	1670	1750
15	4.00	2000	0.021	96	1.4	290	580	1025	1350	1520
16	4.00	2000	.045	182	3.1	200	370	690	1090	1310
17	4.00	2000	.080	299	5.4	150	290	475	750	1050
18	4.00	2000	.168	587	11.4	110	210	340	480	710
Configuration 3: 0.062-inch (0.16-cm) continuous slot							Axial hot gas temperature profile, °F			
19	4.00	2000	0.0	0.0	0.0	---	1450	1625	1775	1830
20	4.00	2000	0.082	823	13.8	200	475	710	950	1160
21	4.00	2000	.042	453	7.1	250	600	950	1300	1500
Configuration 4: 0.062-inch (0.16-cm) continuous slot raised 1/4 inch (0.64 cm) above surface							Axial hot gas temperature profile, °F			
22	4.00	2000	0.0	0.0	0.0	---	1475	1650	1750	1830
23	4.00	2000	0.080	803	13.5	200	400	580	815	1115
24	4.00	2000	.042	454	7.1	250	500	870	1200	1450
Configuration 5: eight 1 4-inch (0.64-cm) holes at 45°							Axial hot gas temperature profile, °F			
25	4.00	2000	0.0	0.0	0.0	---	1320	1550	1700	1800
26	4.00	2000	0.023	164	2.4	290	600	1050	1390	1550
27	4.00	2000	.043	282	4.5	230	435	790	1160	1390
28	4.00	2000	.082	530	8.6	220	345	550	880	1150
29	4.00	2000	.164	967	17.3	160	250	385	540	780

TABLE III. - Continued. LINER FILM COOLING DATA

(a) Concluded. U.S. Customary units

Run	Mass flow rate of hot stream, lb/sec	Combustor exit temperature, °F	Mass flow rate of cooling air, lb/sec	Slot velocity, ft/sec	Mass flux ratio at x = 1 in.	Inlet cooling air temperature, °F	Wall temperature, °F, at specified downstream distances in inches			
							1.0	2.0	3.0	4.0
Configuration 6: four 1/4-inch (0.64-cm) holes at 45°							Axial hot gas temperature profile, °F			
30	4.00	2000	0.0	0.0	0.0	---	1420	1595	1730	1850
31	4.00	2000	0.170	1245	35.8	190	280	410	580	815
32	4.00	2000	.042	591	8.8	280	501	885	1250	1480
33	4.00	2000	.022	339	4.6	350	690	1150	1450	1620
34	3.00	2000	.027	406	7.6	330	590	900	1250	1480
35	3.00	2000	.042	601	11.8	292	500	775	1090	1335
Configuration 6: four 1/4-inch (0.64-cm) holes at 45°							Axial hot gas temperature profile, °F			
36	4.0	1600	0.0	0.0	0.0	---	1200	1340	1470	1590
37	4.0	1600	0.042	595	8.8	285	475	720	1025	1330
Configuration 6: four 1/4-inch (0.64-cm) holes at 45°							Axial hot gas temperature profile, °F			
38	4.0	1400	0.0	0.0	0.0	---	980	1120	1230	1330
39	4.0	1400	0.042	579	8.8	265	435	615	855	1045
Configuration 6: four 1/4-inch (0.64-cm) holes at 45°							Axial hot gas temperature profile, °F			
40	4.0	600	0.0	0.0	0.0	---	595	595	595	595
41	4.0	600	0.042	571	8.8	255	310	410	480	520
Configuration 7: 19 1/16-inch (0.16-cm) holes at 45°							Axial hot gas temperature profile, °F			
42	4.0	2000	0.0	0.0	0.0	---	1395	1570	1710	1850
43	4.0	2000	0.024	1111	17.1	260	660	1060	1375	1580
44	4.0	2000	.043	1269	30.6	215	490	800	1200	1360
45	4.0	2000	.082	1241	58.3	185	360	600	900	1150
46	4.0	2000	.164	1197	116.6	140	280	415	620	820
Configuration 8: eight 3/16-inch (0.48-cm) holes at 0°							Axial hot gas temperature profile, °F			
47	4.0	2000	0.0	0.0	0.0	---	1530	1650	1800	1920
48	4.0	2000	0.167	1362	31.2	320	450	650	850	1040
49	4.0	2000	.084	1219	15.7	400	550	800	1130	1360
50	4.0	2000	.042	638	7.8	440	690	1050	1350	1570
Configuration 9: eight 3/16-inch (0.48-cm) holes at -45°							Axial hot gas temperature profile, °F			
51	4.0	2000	0.0	0.0	0.0	---	1500	1650	1800	1890
52	4.0	2000	0.165	1245	30.8	190	335	460	650	890
53	4.0	2000	.083	994	15.5	250	430	630	930	1180
54	4.0	2000	.043	551	8.0	300	564	945	1300	1520
Configuration 10: wiggle strip in 0.3-inch (0.76-cm) slot							Axial hot gas temperature profile, °F			
55	4.00	2000	0.0	0.0	0.0	---	1496	1650	1780	1920
56	4.00	2000	0.168	382	7.1	135	231	360	560	850
57	4.00	2000	.083	197	3.5	160	315	560	900	1210
58	4.00	2000	.040	107	1.7	240	535	920	1250	1500
59	4.00	2000	.023	64	1.0	265	690	1140	1440	1640

TABLE III. - Continued. LINER FILM COOLING DATA

(b) SI units

Run	Mass flow rate of hot stream, kg/sec	Combustor exit temperature, K	Mass flow rate of cooling air, kg/sec	Slot velocity, m/sec	Mass flux ratio at x = 2.5 cm	Inlet cooling air temperature, K	Wall temperature, K. at specified downstream distances in centimeters			
							2.5	5.1	7.6	10.2
Configuration 1: 0.3-inch (0.76-cm) continuous slot							Axial hot gas temperature profile, K			
1	1.81	1256.	0.0	0.0	0.0	-----	800.0	950.0	1041.7	1094.4
2	1.81	1256	0.0721	93	5.6	333.3	375.0	436.1	516.7	625.0
3	1.81	1256	.0386	53	3.0	355.6	427.8	491.7	622.2	811.1
4	1.81	1256	.0204	30	1.6	383.3	494.4	669.4	783.3	922.2
5	1.81	1256	.0100	17	.8	438.9	572.2	766.7	877.8	991.7
Configuration 1: 0.3-inch (0.76-cm) continuous slot							Axial hot gas temperature profile, K			
6	1.81	1367	0.0	0.0	0.0	-----	1038.9	1138.9	1208.3	1261.1
7	1.81	1367	0.0109	17	0.8	397.2	608.3	850.0	1022.2	1133.3
8	1.81	1367	.0200	28	1.6	366.7	500.0	672.2	894.4	1038.9
9	1.81	1367	.0367	49	2.9	347.2	438.9	533.3	700.0	894.4
10	1.81	1367	.0744	95	5.8	330.0	375.0	433.3	533.3	688.9
Configuration 2: 0.156-inch (0.4-cm) continuous slot							Axial hot gas temperature profile, K			
11	1.81	1256	0.0	0.0	0.0	-----	888.9	1000.0	1072.2	1116.7
12	1.81	1256	0.0748	180	11.5	316.7	355.6	422.2	494.4	588.9
13	1.81	1256	.0367	95	5.6	338.9	394.4	477.8	633.3	783.3
Configuration 2: 0.156-inch (0.4-cm) continuous slot							Axial hot gas temperature profile, K			
14	1.81	1367	0.0	0.0	0.0	-----	966.7	1094.4	1183.3	1227.8
15	1.81	1367	0.0095	29	1.4	416.7	577.8	825.0	1005.6	1100.0
16	1.81	1367	.0204	56	3.1	366.7	461.1	638.9	861.1	983.3
17	1.81	1367	.0363	91	5.4	338.9	416.7	519.4	672.2	838.9
18	1.81	1367	.0762	179	11.4	316.7	372.2	444.4	522.2	650.0
Configuration 3: 0.062-inch (0.16-cm) continuous slot							Axial hot gas temperature profile, K			
19	1.81	1367	0.0	0.0	0.0	-----	1061.1	1158.3	1241.7	1272.2
20	1.81	1367	0.0372	251	13.8	366.7	519.4	650.0	783.3	900.0
21	1.81	1367	.0191	138	7.1	394.4	588.9	783.3	977.8	1088.9
Configuration 4: 0.062-inch (0.16-cm) continuous slot raised 1/4 inch (0.64 cm) above surface							Axial hot gas temperature profile, K			
22	1.81	1367	0.0	0.0	0.0	-----	1075.0	1172.2	1227.8	1272.2
23	1.81	1367	0.0363	254	13.5	366.7	477.8	577.8	708.3	875.0
24	1.81	1367	.0191	138	7.1	394.4	533.3	738.9	922.2	1061.1
Configuration 5: eight 1/4-inch (0.64-cm) holes at 45°							Axial hot gas temperature profile, K			
25	1.81	1367	0.0	0.0	0.0	-----	988.9	1116.7	1200.0	1255.6
26	1.81	1367	0.0104	50	2.4	416.7	588.9	838.9	1027.8	1116.7
27	1.81	1367	.0195	86	4.5	383.3	497.2	694.4	900.0	1027.8
28	1.81	1367	.0372	162	8.6	377.8	447.2	561.1	744.4	894.4
29	1.81	1367	.0744	295	17.3	344.4	394.4	469.4	555.6	688.9

TABLE III. - Concluded. LINER FILM COOLING DATA

(b) Concluded. SI units

Run	Mass flow rate of hot stream, kg/sec	Combustor exit temperature, K	Mass flow rate of cooling air, kg/sec	Slot velocity, m/sec	Mass flux ratio at x = 2.5 cm	Inlet cooling air temperature, K	Wall temperature, K, at specified downstream distances in centimeters			
							2.5	5.1	7.6	10.2
Configuration 6: four 1/4-inch (0.64-cm) holes at 45°							Axial hot gas temperature profile, K			
30	1.81	1367	0.0	0.0	0.0	-----	1044.4	1141.7	1216.7	1283.3
31	1.81	1367	0.0771	641	35.8	361.1	411.1	483.3	577.8	708.3
32	1.81	1367	.0191	180	8.8	411.1	536.1	747.2	950.0	1077.8
33	1.81	1367	.0100	103	4.6	450.0	638.9	894.4	1061.1	1155.6
34	1.36	1367	.0122	124	7.6	438.9	583.3	755.6	950.0	1077.8
35	1.36	1367	.0191	183	11.8	417.8	533.3	686.1	861.1	997.2
Configuration 6: four 1/4-inch (0.64-cm) holes at 45°							Axial hot gas temperature profile, K			
36	1.81	1144	0.0	0.0	0.0	-----	922.2	1000.0	1072.2	1138.9
37	1.81	1144	0.0191	181	8.8	413.9	519.4	655.6	825.0	944.4
Configuration 6: four 1/4-inch (0.64-cm) holes at 45°							Axial hot gas temperature profile, K			
38	1.81	1033	0.0	0.0	0.0	-----	800.0	877.8	938.9	994.4
39	1.81	1033	0.0191	177	8.8	402.8	497.2	597.2	730.6	836.1
Configuration 6: four 1/4-inch (0.64-cm) holes at 45°							Axial hot gas temperature profile, K			
40	1.81	589	0.0	0.0	0.0	-----	586.1	586.1	586.1	586.1
41	1.81	589	0.0191	174	8.8	397.2	427.8	483.3	522.2	544.4
Configuration 7: 19 1/16-inch (0.16-cm) holes at 45°							Axial hot gas temperature profile, K			
42	1.81	1367	0.0	0.0	0.0	-----	1030.6	1127.8	1205.6	1283.3
43	1.81	1367	0.0109	339	17.1	400.0	622.2	844.4	1019.4	1133.3
44	1.81	1367	.0195	569	30.6	375.0	527.8	700.0	922.2	1052.8
45	1.81	1367	.0372	1037	58.3	358.3	455.6	588.9	755.6	894.4
46	1.81	1367	.0744	1929	116.6	333.3	411.1	486.1	600.0	711.1
Configuration 8: eight 3/16-inch (0.48-cm) holes at 0°							Axial hot gas temperature profile, K			
47	1.81	1367	0.0	0.0	0.0	-----	1105.6	1172.2	1255.6	1322.2
48	1.81	1367	0.0758	670	31.2	433.3	505.6	616.7	727.8	833.3
49	1.81	1367	.0381	372	15.7	477.8	561.1	700.0	883.3	1011.1
50	1.81	1367	.0191	194	7.8	500.0	638.9	838.9	1005.6	1127.8
Configuration 9: eight 3/16-inch (0.48-cm) holes at -45°							Axial hot gas temperature profile, K			
51	1.81	1367	0.0	0.0	0.0	-----	1088.9	1172.2	1255.6	1305.6
52	1.81	1367	0.0748	552	30.8	361.1	441.7	511.1	616.7	750.0
53	1.81	1367	.0376	303	15.5	394.4	494.4	605.6	772.2	911.1
54	1.81	1367	.0195	168	8.0	422.2	569.4	780.6	977.8	1100.0
Configuration 10: wiggle strip in 0.3-inch (0.76-cm) slot							Axial hot gas temperature profile, K			
55	1.81	1367	0.0	0.0	0.0	-----	1086.1	1172.2	1244.4	1322.2
56	1.81	1367	0.0762	117	7.1	330.6	383.3	455.6	566.7	727.8
57	1.81	1367	.0376	60	3.5	344.4	430.6	566.7	755.6	927.8
58	1.81	1367	.0181	33	1.7	388.9	552.8	766.7	950.0	1088.9
59	1.81	1367	.0104	19	1.0	402.8	638.9	888.9	1055.6	1166.7

46

REFERENCES

1. Eckert, E. R. G.; and Birkebak, R. C.: The Effects of Slot Geometry on Film Cooling. Heat Transfer, Thermodynamics, and Education. Harold A. Johnson, ed., McGraw-Hill Book Co., Inc., 1964, pp. 150-163.

2. Stollery, J. L.; and El-Ehwany, A. A. M.: A Note on the Use of a Boundary-Layer Model for Correlating Film-Cooling Data. Int. J. Heat & Mass Transfer, vol. 8, no. 1, Jan. 1965, pp. 55-65.

3. Hatch, James E.; and Papell, S. Stephen: Use of a Theoretical Flow Model to Correlate Data for Film Cooling or Heating an Adiabatic Wall by Tangential Injection of Gases of Different Fluid Properties. NASA TN D-130, 1959.

4. Spalding, D. B.: Prediction of Adiabatic Wall Temperatures in Film-Cooling Systems. AIAA J., vol. 3, no. 5, May 1965, pp. 965-967.

5. Kutateladze, S. S.; and Leontev, A. I.: The Heat Curtain in the Turbulent Boundary Layer of a Gas. High Temp., vol. 1, no. 2, Sept.-Oct. 1963, pp. 250-258.

6. Carlson, L. W.; and Talmor, E.: Gaseous Film Cooling at Various Degrees of Hot-Gas Acceleration and Turbulence Levels. Int. J. Heat & Mass Transfer, vol. 11, no. 11, Nov. 1968, pp. 1695-1713.

7. Humenik, Francis M.: Performance of Short Length Turbojet Combustor Insensitive to Radial Distortion of Inlet Airflow. NASA TN D-5570, 1970.

8. Kacker, S. C.; and Whitelaw, J. H.: The Effect of Slot Height and Slot-Turbulence Intensity on the Effectiveness of the Uniform Density, Two-Dimensional Wall Jet. J. Heat Transfer, vol. 90, no. 4, Nov. 1968, pp. 469-475.

9. Metzger, D. E.; and Fletcher, D. D.: Surface Heat Transfer Immediately Downstream of Flush, Non-Tangential Injection Holes and Slots. Paper 69-523, AIAA, June 1969.

10. Wieghardt, K.: Hot-Air Discharge for De-Icing. Trans. F-TS-919-RE, Army Air Forces, Air Material Command, Dec. 1946. (Ueber das Ausblasen von Warmluft fuer Enteiser.)

11. Anon.: Computer Program for the Analysis of Annular Combustors. Vol. 1: Calculation Procedures. 1111-1, Northern Research and Eng. Corp. (NASA CR-72374), Jan. 29, 1968.

12. Sturgess, Geoffrey J.: Comment on "Prediction of Adiabatic Wall Temperatures in Film-Cooling Systems." AIAA J., vol. 4, no. 4, Apr. 1966, pp. 763-765.

13. Schlichting, Hermann (J. Kestin, trans.): Boundary-Layer Theory. Sixth ed., McGraw-Hill Book Co., Inc., 1968.

1. Report No. NASA TN D-6360	2. Government Accession No.	3. Recipient's Catalog No.
4. Title and Subtitle COMBUSTOR LINER FILM COOLING IN THE PRESENCE OF HIGH FREE-STREAM TURBULENCE		5. Report Date July 1971
		6. Performing Organization Code
7. Author(s) Albert J. Juhasz and Cecil J. Marek		8. Performing Organization Report No. E-6135
9. Performing Organization Name and Address Lewis Research Center National Aeronautics and Space Administration Cleveland, Ohio 44135		10. Work Unit No. 720-03
		11. Contract or Grant No.
		13. Type of Report and Period Covered Technical Note
12. Sponsoring Agency Name and Address National Aeronautics and Space Administration Washington, D.C. 20546		
		14. Sponsoring Agency Code

15. Supplementary Notes

16. Abstract

Film cooling effectiveness data for various slot geometries were obtained using an instrumented liner installed in a rectangular sector of a gas turbine combustor. Because of the high combustor free-stream turbulence, experimental film cooling effectiveness values were considerably lower than those predicted by several correlations currently in use. To improve prediction accuracy, a simple mixing model was developed which takes into account the turbulence level of the hot gas stream. This model adequately correlated the data of this report and also the low turbulence duct data of two references in the literature.

17. Key Words (Suggested by Author(s)) Film cooling Turbulence Combustor	18. Distribution Statement Unclassified - unlimited		
19. Security Classif. (of this report) Unclassified	20. Security Classif. (of this page) Unclassified	21. No. of Pages 50	22. Price* $3.00